EJSDR
European Journal of Sustainable Development Research
e-ISSN : 2458-8091

K-Nearest Neighbors as a Transparent Baseline for Automated EEG Sleep Staging

Ahmet Sertol Köksal[1]*
[1]*Yozgat Bozok University, Department of Computer Engineering, 66100, Yozgat, Turkey.*
**Corresponding Author email: ahmet.koksal@bozok.edu.tr*

Abstract

Sleep staging plays a key role in evaluating sleep health, but manually annotating polysomnography data is both time-consuming and prone to inconsistencies. This study presents the first comprehensive baseline evaluation of the K-Nearest Neighbors algorithm for EEG-based sleep staging, using a nested subject-wise cross-validation approach. We assessed 24 configurations combining six data scalers and four distance metrics on the ISRUC dataset. Overall, KNN delivered stable performance, with macro-F1 scores between 0.59 and 0.62 and Cohen's κ ranging from 0.55 to 0.57. Among scalers, the Normalizer consistently performed the worst (macro-F1≈0.52), while Power transform, Standard, and Quantile scalers produced more reliable outcomes. The choice of distance metric had a relatively minor impact, but Euclidean distance offered the best trade-off—slightly improving accuracy while delivering runtimes up to five times faster than Cosine. Hyperparameter tuning consistently favored $k \approx 30$ with distance weighting, indicating that extensive parameter searches may not be necessary. At the individual class level, Wake (F1≈0.79) and N3 (F1≈0.82) stages were identified with high accuracy, whereas N2 (F1≈0.68) was moderately accurate. REM (F1≈0.56) and particularly N1 (F1≈0.27) remained difficult to classify, though some setups improved performance by up to 8%. In summary, while KNN does not match deep learning in raw accuracy, it provides valuable benefits in terms of transparency, reproducibility, and interpretability. We recommend using Euclidean distance, k≈30 with distance weighting, and avoiding the Normalizer as a practical and interpretable baseline for future EEG-based sleep analysis.

Key words

Distance metric, EEG, KNN, Sleep staging

1. INTRODUCTION

Sleeping is a biological phenomenon central to all humans, and accurate evaluation is essential in clinical diagnosis and in understanding human health. Although the sleep monitoring gold standard, polysomnography (PSG), involves time-consuming, scorer variability-prone by-hand annotation of 30-second epochs into stages (Wake, N1, N2, N3, REM), these concerns have motivated development over recent years of automated sleep staging methods, from classical machine learning (ML) through recent deep learning (DL) methods. DL models, despite attainable accuracy levels impressive on paper [1-4], typically necessitate considerable computational power, complex designs, and are in large part "black-box" systems, thus limiting reproducibility and interpretability in clinical use. In contrast, simpler ML methods [5-8] are more interpretable, computationally

lightweight, and capable, in certain conditions, of producing robust results with modest datasets, at points reaching accuracy levels close to DL systems.

Out of these methodologies, the K-Nearest Neighbors algorithm provides a natural baseline. KNN is intuitive, instance-based, and was successfully implemented in a wide variety of application domains. However, accuracy is well known to be significantly impacted by scaling, distance measure, and hyperparameters such as k-neighbors and weighting. Several case studies in a variety of application domains have demonstrated that choice of distance measure can significantly impact classification decisions. Abualfeilat et al. [9], for example, reported that careful selection of metric provided better predictive power in healthcare applications. Ma et al. [10] noted that alternative metrics, namely Minkowski, surpassed the usual Euclidean distance in tasks in the application domain of medical imaging. Mladenova and Valova [11] compared several distance functions in a systematic case study on text classification and confirmed that choice of metric significantly interacted with properties within the features, but noted that preprocessing by normalization impacted the results as well. Accordingly, Zhang et al. [12] suggested hybrid distance functions and demonstrated that combining metrics can remove ambiguities happening in the case of multiple equi-distance neighbors. In conclusion, the above case studies confirm that accuracy in KNN is significantly linked with distance measure choice.

In spite of all this, nothing is well established regarding the effect of distance metrics on KNN in particular in EEG-based sleep staging. To our knowledge, there are barely any works tackling the former, notably the paper by Qureshi et al. [13], comparing Euclidean, Manhattan, and Chebyshev distance in a pilot study with 25 subjects and 10-fold cross-validation. This, however, was a restricted study in several important aspects: it did not do subject-wise data division, it was restricted to a single scaling method, and it did not methodically search hyperparameters such as k or weighting. Hence, the collective influence of scaling, metric choice, and weight giving to neighbors has never been seriously taken into account, and thus a seminal methodological fallacy in the field goes undetected.

This disparity suggests the need for a systematic and reproducible investigation into KNN settings in the context of EEG-based sleep stage classification. In the paper, we close that gap by comparing six scalers and four distance functions in 24 combinations on the ISRUC dataset (100 subjects, 1-channel EEG). The rigoruous nested subject-wise cross-validation scheme was applied in order to avoid leakage, and both the performance (macro-F1, Cohen's Kappa, per-class F1) and the computational cost were evaluated. Rather than comparing against deep learning systems, we strive at presenting a systematic and reproducible KNN baseline. Through insights on how scaling, choice of metric, and hyperparameters affect results, we provide practical suggestions on how to set up KNN, thereby offering a reference point in itself in the way of methodological improvement in the future as well as a useful tool in applied practice, in situations in which simplicity, interpretability, and efficiency are paramount. This baseline is most useful in low-resource clinical settings and in wearable or home monitoring settings, in which the depth and resource intensity of deep learning systems are infeasible.

2. MATERIALS AND METHODS

An easy way to comply with the symposium paper formatting requirements is to use this document as a template and simply type your text into it.

2.1. Dataset

We used the ISRUC-Sleep dataset [14], providing polysomnography recordings during a complete night in 100 participants. A single overnight EEG was employed in each person. Segmentation was performed on epochs in 30 seconds, consistent with established sleep stage practice. The initial sample frequency was 200 Hz but was reduced by half, i.e., 100 Hz, in order to reduce the computational burden. Since a low-cost, single-channel setting was aimed at and existing works made comparable, a single EEG channel, i.e., C4–A1, was used. Artifact rejection and band-pass filtering were noted as performed during dataset preparation and therefore no further preprocessing was needed.

2.2. Feature Engineering and Selection

40 candidate features were computed on a 30-second basis from every epoch during statistical, spectral, and nonlinear domains (Supplementary Table S1). Feature selection was performed with a combined correlation, information-theoretic, and model-based method. The overall process is described in Supplementary Section S1. Following selection, 15 features were retained in ISRUC (Supplementary Table S2).

2.3. Modeling and Evaluation

We utilized a KNN classifier in order to compare the effect of preprocessing and distance functions on sleep staging based on EEG recordings. We compared six scalers, namely Standard (STD), Robust (ROB), MinMax

(MMX), Quantile (QNT), Power Transform (Yeo Johnson) (PYJ), and Normalizer (NRM), and four distance functions were used in each scaler, namely Euclidean (EUC), Manhattan (MAN), Chebyshev (CHB), and Cosine (COS). This experimental setup resulted in a total of 24 scalar–metric combinations. For all configurations, we tuned the value of the number of neighbors k in the range 1--50, and both uniform and distance weighting schemes were used.

The model was evaluated by a nested cross-validation scheme. The outer loop utilized a 20-fold subject-wise cross-validation in order to obtain unbiased estimates of the generalization error. A 3-fold subject-wise cross-validation was utilized in the inner loop in order to optimize the hyperparameters. Both loops used strict subject separation in order to prevent data leakage, thus no epoch coming from the same individual was present simultaneously in both train and test folds. The same care was also taken in preprocessing: all scalers were trained only on the train folds and then applied on the corresponding test ones, in order to prevent distributional information leakage.

Hyperparameter optimization (HPO) was carried out through Optuna [15]. The optimization was configured to run 60 trials per (fold, scaler, metric) combination, and we chose the Tree-structured Parzen Estimator [16] as the sampler along with Successive Halving [17] as a pruning strategy. The first 12 iterations were left as exploration in order to enjoy enough diversity in candidate solutions. The above settings made it efficient in search without redundant computation. Interestingly, the optimization was always converging towards $k \approx 30$ with distance weighting, a fact on which we comment in the Results section.

We assessed mainly through the use of macro-F1 and Cohen's Kappa. We chose macro-F1 as the primary metric as it treats minority classes such as N1 and REM in a balanced fashion, and we included Kappa as it has been adopted as a de facto standard in sleep stage classification. We also provided extra measures, accuracy, precision, recall, and per-class F1 scores, in order to provide a fuller accounting of a joint accuracy and cost profile. We compared computational efficiency in terms of HPO time, time to fit model, time to make a prediction, and overall runtime per configuration, and thus a joint evaluation of accuracy and cost is possible.

2.4. Implementation Details

All the calculations were performed in Python (3.12.3). The machine learning experiments were implemented in scikit-learn (1.6.1). The data manipulations and numerical computations were performed in Pandas (2.2.3) and NumPy (1.26.4), respectively. All the experiments were conducted on a Windows 11 Pro computer running on a 12th Gen Intel(R) Core(TM) i9-12900 CPU (2.40 GHz) and 128 GB RAM. Training and validation were done exclusively on CPU and without a GPU.

3. RESULTS & DISCUSSION

All paragraphs must be justified, i.e. both left-justified and right-justified.

3.1. Overall Performance

To illustrate the distribution of performance on scaler–metric combinations, we give a sample subset of the results on macro-F1 and Kappa in Table 1, presenting the three highest ranked combinations and MMX and NRM as a reference, and results of all 24 combinations in detail in Supplementary Table S3.

As seen in Table 1, macro-F1 values fell within a narrow band of approximately 0.59–0.62, representing a difference of approximately 5%. The confidence intervals overlap significantly. Although this implies that the choice of scaler and metric has limited statistical significance on performance, the range of results is not entirely uniform. PYJ and QNT were the best performing scalers, followed closely by STD and ROB. MMX lagged slightly behind, and NRM consistently underperformed.

Table 1. Representative subset of scaler–metric combinations with macro-F1 and Kappa results.

Scaler	Metric	Macro-F1 (mean ± CI95)	Kappa (mean ± CI95)
PYJ	EUC	0.620 ± 0.017	0.577 ± 0.021
PYJ	MAN	0.619 ± 0.017	0.576 ± 0.021
QNT	EUC	0.618 ± 0.016	0.576 ± 0.020
MMX	MAN	0.598 ± 0.016	0.548 ± 0.021
NRM	MAN	0.540 ± 0.020	0.487 ± 0.024

Among scalers, strongly similar results were obtained by PYJ, STD, QNT, and ROB (≈0.60–0.62), and MMX was somewhat lagging (≈0.59), yet statistically within the same group as the leaders. The outlier was NRM, producing significantly lower results (macro-F1 ≈0.52–0.53, with non-overlapping CI95).

In distance calculations, EUC, MAN, CHB, and COS all behaved alike (≈0.59–0.60). Statistically significant differences were indicated by Friedman's test ($\chi^2 = 280.6, p < 10^{-45}$), but in light of the small absolute effect sizes, practical significance is restricted.

In addition to F1, we also examined Cohen's Kappa, a popular choice in sleep stage classification. Estimations of Kappa were also strongly and invariably in the range 0.55–0.57 over scaler–metric pairs, with minor variations and overlapping intervals of confidence. Following the Landis & Koch scale [18], this corresponds to moderate agreement, in that, despite KNN providing a workable baseline, it does not reach levels typically desired in clinical-grade systems of "substantial" agreement. Our findings then confirm that Kappa mirrors the F1 findings: differences in performance are small over preprocessing decisions, with NRM continuing to underperform.

Figure 1 heatmap visualizations and Figure 2 grouped bar charts ((a) and (b)) also confirm these findings, demonstrating consistency in performance across scaler–metric combinations. NRM is consistently lagging in all the visualizations, confirming the conclusion that preprocessing and metric choice are not decisive in overall performance.

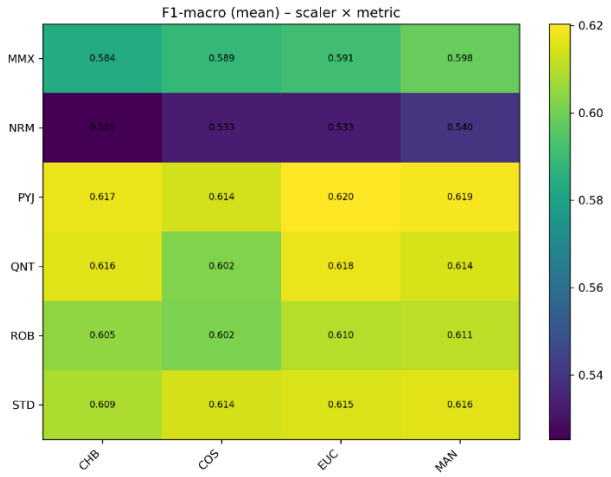

Figure 1. Heatmap of macro-F1 scores across all scaler–metric combinations.

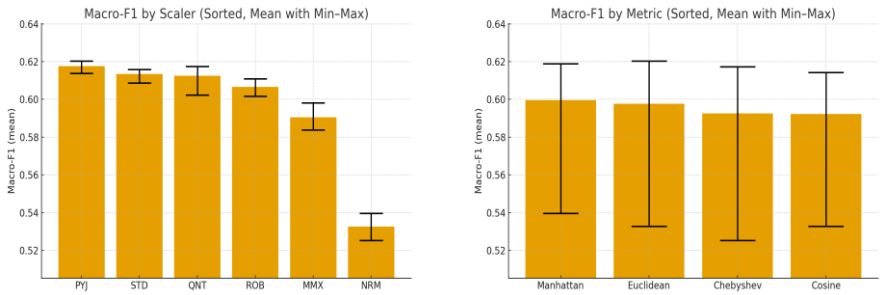

Figure 2. (a) Bar chart of best-performing metric per scaler. (b) Bar chart of best-performing scaler per metric.

3.2. Stability Across Folds

At the fold level, it was observed that variability was low, and the standard deviations lay within 0.036–0.041 and CV% lay within 5–7% among all strong scalers. Again, NRM did not only underperform but also exhibited the highest variability (CV% ≈9), a fact that both indicates instability and inaccuracy.

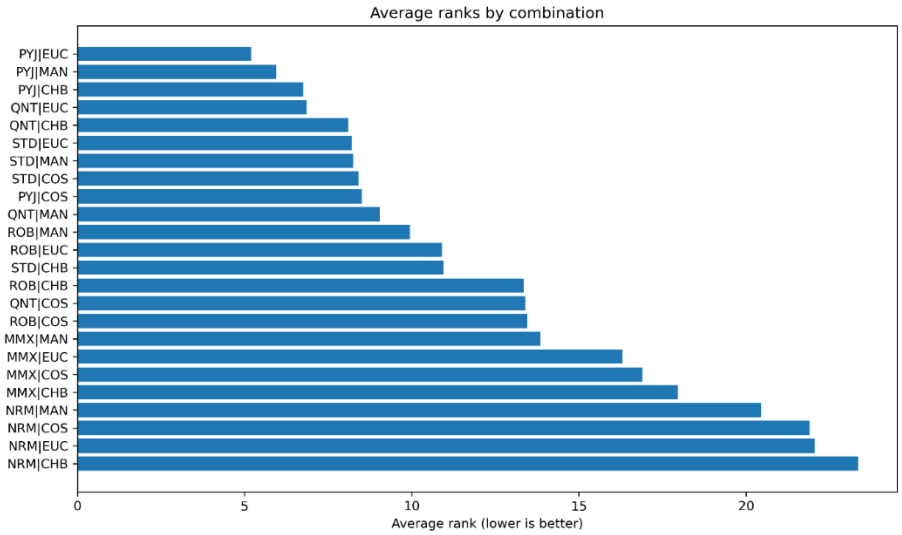

Figure 3. Average ranks of scaler–metric combinations across 20 folds.

Average rank analysis (Figure 3) supported the above results also: PYJ and QNT were first overall, STD and ROB were in a close position, MMX trailed a pace, and NRM was consistently the poorest.

The main effect tests confirmed these trends. As Figures 2 (a) and (b) show, scalers are highly precise in their segregation (PYJ, STD, QNT, ROB all close together, MMX fairly weak, and NRM well down), and metrics generate roughly equal means (MAN, EUC, CHB, COS ~0.59–0.60).

3.3. Class-wise Performance

Class-level analysis offered a less sensationalistic description. The total macro-F1 changes were minuscule, yet in all the classes the optimal combination was evident.

Table 2. Best scaler–metric combination per class based on macro-F1.

Class	Best combo	F1
N3	PYJ+COS	0.815
W	STD+EUC	0.792
N2	QNT+CHB	0.679
REM	PYJ+MAN	0.556
N1	STD+EUC	0.276

As seen in Table 2, the model had little trouble identifying N3 (F1 = 0.815) and Wake (F1 = 0.792), both of which were detected with high confidence. N2 was somewhat less accurate (F1 = 0.679), but still reasonable. In contrast, REM (F1 = 0.556) and especially N1 (F1 = 0.276) proved much harder for the model to classify correctly.

For N1, there was low recall (~0.21), but higher precision (~0.40), as if the model rarely made N1 predictions but was quite precise in so doing. The 0.25 vs 0.27 F1 discrepancy appears minuscule in absolute form, but represents ≈8% relative improvement, a potentially large impact in clinical or application settings. This shows that no scaling or choice of metric on its own can adequately address the problem of classifying N1/REM. However, the modest gains observed with certain combinations (e.g., STD+EUC being somewhat effective on N1) potentially could be a significant point of departure if supplemented with certain preprocessing or augmentation strategies particular to each class.

In order to achieve full transparency, the class-wise results on all combinations of scalers and metrics are presented in the Supplementary Table S4. This table shows, e.g., that NRM delivers significantly worse performance for N1 (≈0.18), while all other scalers are closely clustered around 0.25–0.27. This verifies the

above conclusion that NRM is consistently inferior, while the remaining scalers and metrics are different from one another insignificantly.

3.4. Timing and Computational Cost

The timing analysis indicated that unless accuracy relies on metrics, they contribute substantially to computation time. Figure 4 provides a summary in grouped bar plots, in which a group represents a scaler and four distance measures are shown as adjacent bars. The three panels are displayed in a row and are associated with HPO time, fit time, and runtime in total.

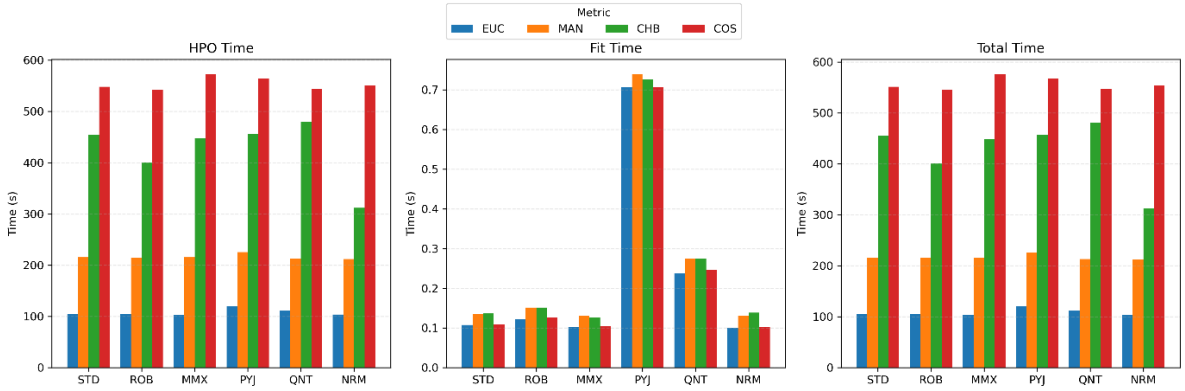

Figure 4. Grouped bar plots of HPO, fit, and total runtime across scaler–metric combinations.

EUC was by far the fastest, with total runtime from ~105–122 s. MAN took approximately 210–224 s (~2× slower), CHB 420–515 s (~4× slower), and COS was the slowest at ~550–590 s (~5–6× slower). The predictor time was also comparable in trend (EUC≈0.15 s, COS≈3.4 s). Among scalers, PYJ took a somewhat larger fitting overhead (~0.7 s compared to 0.1–0.3 s), but total runtime was nevertheless predominantly determined by the choice of metric rather than scaler.

The bar charts in Figure 5 clearly illustrate these differences: COS is the costliest option, while EUC has the same prediction accuracy at much less cost. Because it offers a balanced solution between performance and computational efficiency, we recommend that EUC be the default choice in resource-constrained environments.

3.5. Hyperparameter Optimization

The HPO results were remarkably consistent: (i) The optimal k-value was almost always 31; interquartile ranges across folds were narrow (IQR≤2.5). (ii) "weights = distance" was mostly superior; uniform weighting was rarely chosen but never among the best. (iii) For NRM, k ranged from 15–21 but always performed poorly. These observations demonstrate that KNN can be used as a consistent and computationally efficient baseline for EEG sleep staging.

3.6. Limitations

This study has several limitations. First, the analysis was conducted only on the ISRUC dataset; therefore, the generalizability of the findings to other datasets may be limited. Second, only a single EEG channel was used, which limits spatial information. Third, only 40 features were extracted from the EEG data, which may prevent the model from reflecting potential insights from a broader feature space. Finally, no data augmentation strategy was implemented, which limits classification performance from reaching optimal levels, particularly for minority classes such as N1 and REM.

3.7. Future Work

In light of the noted limitations, it will be important for future studies to validate on different datasets and modalities. Class-specific strategies should be investigated to improve the underperformance, particularly in the N1 and REM stages. For this purpose, advanced feature engineering, cost-sensitive learning, and data augmentation methods appear promising. Furthermore, the performance of different distance metrics such as Mahalanobis and Braycurtis can be evaluated. Tests on large-scale databases such as Sleep-EDF and MASS will also demonstrate the robustness of the proposed approach. Finally, the methods we use here—specifically, subject-wise cross-validation and data leakage prevention—may also provide a useful framework for algorithms other than KNN.

4. CONCLUSIONS

This study presented a baseline analysis of KNN in EEG-based sleep staging for 24 combinations of 6 scalers and 4 distance metrics. Data leakage was prevented in the analyses using extensive nested cross-validation. For most combinations, performance differences were small. The Normalizer scaler consistently performed poorly, while the other scalers were similar. The Quantile scaler provided more consistent results, while the Standard scaler produced a more balanced picture across classes. While there were minor differences between scalers, the overall performance was primarily determined by the algorithm's structure.

The effect of distance metrics on classification performance was also limited. The Euclidean distance was both more accurate and significantly faster than alternatives such as Cosine. Therefore, it offered the best balance between accuracy and speed. Runtime analysis showed that the Power transform scaler had the worst fit-time performance. There were no significant differences for the other scalers. The choice of distance metric was crucial in terms HPO time. Metrics other than Euclidean were more costly. For HPO, the weighting setting should definitely be "distance"; the number of neighbors should be approximately 30. It can be argued that further parameterization is often unnecessary.

Class-based results showed that Wake and N3 are more easily distinguished, while N1 and REM are difficult to predict. While the scaler and metric combinations offered small absolute gains, especially for N1, the relative increase of 8% can be meaningful in practice.

In conclusion, this study establishes a transparent and reproducible KNN baseline for EEG sleep staging. With distance-based weighting, approximately 30 neighbors and Euclidean distance are strongly recommended as a default choice. Furthermore, Power transform and Quantile scalers can be used to improve overall performance, while the Standard scaler is preferred in resource-constrained situations. The Normalizer scaler is not recommended. These findings provide a reliable reference for future comparative studies in the field of KNN EEG sleep staging.

ACKNOWLEDGMENT

This work has been supported by Yozgat Bozok University Scientific Research Projects Coordination Unit under grant number FED-2025-1548.

CONFLICT OF INTEREST STATEMENT

The author declares that there is no conflict of interest.

REFERENCES

[1]. H. Phan, K. P. Lorenzen, E. Heremans, O. Y. Chén, M. C. Tran, P. Koch, and M. De Vos, “L-SeqSleepNet: Whole-cycle long sequence modeling for automatic sleep staging,” *IEEE Journal of Biomedical and Health Informatics,* vol. 27, no. 10, pp. 4748–4757, 2023.

[2]. M. Perslev, S. Darkner, L. Kempfner, M. Nikolic, P. J. Jennum, and C. Igel, “U-Sleep: resilient high-frequency sleep staging,” *NPJ Digital Medicine,* vol. 4, no. 1, p. 72, 2021.

[3]. A. Supratak and Y. Guo, “TinySleepNet: An efficient deep learning model for sleep stage scoring based on raw single-channel EEG,” in *Proc. 42nd Annu. Int. Conf. IEEE Eng. Med. Biol. Soc. (EMBC),* Jul. 2020, pp. 641–644.

[4]. H. Phan, K. Mikkelsen, O. Y. Chén, P. Koch, A. Mertins, and M. De Vos, “Sleeptransformer: Automatic sleep staging with interpretability and uncertainty quantification,” *IEEE Trans. Biomed. Eng.,* vol. 69, no. 8, pp. 2456–2467, 2022.

[5]. C. H. Tai, T. Y. Liao, S. P. Chen, and M. H. Chung, “Sleep stage classification using light gradient boost machine: exploring feature impact in depressive and healthy participants,” *Biomed. Signal Process. Control,* vol. 88, p. 105647, 2024.

[6]. S. K. Satapathy, D. Loganathan, and P. Narayanan, “Automated sleep staging analysis using sleep EEG signal: A machine learning based model,” in *Proc. Int. Conf. Advance Comput. Innovative Technol. Eng. (ICACITE),* Mar. 2021, pp. 87–96.

[7]. E. Moris and I. Larrabide, “Evaluating sleep-stage classification: how age and early-late sleep affects classification performance,” *Med. Biol. Eng. Comput.,* vol. 62, no. 2, pp. 343–355, 2024.

[8]. S. K. Satapathy and D. Loganathan, “Multimodal multiclass machine learning model for automated sleep staging based on time series data,” *SN Comput. Sci.,* vol. 3, no. 4, p. 276, 2022.

[9]. H. A. Abu Alfeilat, A. B. Hassanat, O. Lasassmeh, A. S. Tarawneh, M. B. Alhasanat, H. S. E. Salman, and V. S. Prasath, "Effects of distance measure choice on k-nearest neighbor classifier performance: a review," *Big Data,* vol. 7, no. 4, pp. 221–248, 2019.
[10]. X. Ma, X. Han, and L. Zhang, "An improved k-nearest neighbor algorithm for recognition and classification of thyroid nodules," *J. Ultrasound Med.,* vol. 43, no. 6, pp. 1025–1036, 2024.
[11]. T. Mladenova and I. Valova, "Analysis of the KNN classifier distance metrics for Bulgarian fake news detection," in *Proc. 3rd Int. Congr. Human-Computer Interaction, Optimization Robotic Appl. (HORA),* Jun. 2021, pp. 1–4.
[12]. C. Zhang, P. Zhong, M. Liu, Q. Song, Z. Liang, and X. Wang, "Hybrid metric K-nearest neighbor algorithm and applications," *Math. Probl. Eng.,* vol. 2022, no. 1, p. 8212546, 2022.
[13]. S. Qureshi, S. Karrila, and S. Vanichayobon, "Human sleep scoring based on K-nearest neighbors," *Turk. J. Electr. Eng. Comput. Sci.,* vol. 26, no. 6, pp. 2802–2818, 2018.
[14]. S. Khalighi, T. Sousa, J. M. Santos, and U. Nunes, "ISRUC-Sleep: A comprehensive public dataset for sleep researchers," *Comput. Methods Programs Biomed.,* vol. 124, pp. 180–192, 2016.
[15]. T. Akiba, S. Sano, T. Yanase, T. Ohta, and M. Koyama, "Optuna: A next-generation hyperparameter optimization framework," in *Proc. 25th ACM SIGKDD Int. Conf. Knowl. Discov. Data Mining,* Jul. 2019, pp. 2623–2631.
[16]. J. Bergstra, R. Bardenet, Y. Bengio, and B. Kégl, "Algorithms for hyper-parameter optimization," in *Proc. 24th Int. Conf. Neural Inf. Process. Syst. (NeurIPS),* Granada, Spain, Dec. 2011, pp. 2546–2554.
[17]. K. Jamieson and A. Talwalkar, "Non-stochastic best arm identification and hyperparameter optimization," in *Proc. 19th Int. Conf. Artif. Intell. Statist. (AISTATS),* vol. 51, A. Gretton and C. C. Robert, Eds. PMLR, 2016, pp. 240–248.
[18]. J. R. Landis and G. G. Koch, "The measurement of observer agreement for categorical data," *Biometrics,* vol. 33, no. 1, pp. 159–174, 1977.

EJSDR
European Journal of Sustainable Development Research
e-ISSN : 2458-8091

Proposal for a World Energy Stock Balance Sheet

Michael Bosch[1]*
[1]*Albstadt-Sigmaringen University, Life-Sciences Faculty, D-72488 Sigmaringen, Germany*
**Corresponding Author email: boschm@hs-albsig.de*

Abstract

Considering the sharp increase in global energy demand, the question arises whether worldwide energy resources will be sufficient to cover humankind's future energy requirements (including energy for food requirements). In addition to the urgent built up of renewable energy systems, energy-intensive processes to prevent greenhouse gases from being released into the atmosphere (Carbon Capture and Storage, CCS) or removed from there (Carbon Dioxide Removal, CDR, in particular Direct Air Capture, DAC) are required to meet the climate targets. On the basis of a comprehensive analysis of existing Systems of Environmental Economic Accounting (SEEA) and the International Recommendations for Energy Statistics (IRES), a proposal for a World Energy Stock Balance Sheet (WESBS) consistent with these systems was developed. The principle of prudent valuation, borrowed from business accounting, was also applied, which requires the inclusion of energy consumption for CCS and DAC. The assets side of the WESBS shows all fossil and renewable primary, secondary and final energy sources at the balance sheet date prudently valued with the energy unit Peta Joule (PJ). Provisions for the energy losses in PJ that would arise when the capitalized primary, secondary and final energy stocks are converted into useful energy are shown on the liability side of the WESBS, as well as provisions for the energy consumption for CCS and DAC. The respective energy consumption is calculated by first applying Life Cycle Assessment (LCA) emission factors to calculate the greenhouse gas emissions and thereafter using LCA energy consumption factors of CCS or DAC. The difference between energy assets and energy liabilities results in the energy equity in PJ, which is available for the future useful energy demand of humankind under the precondition that the climate targets are met. This paper explains the items of the proposed WESBS and the developed valuation methods in appropriate detail.

Key words

World Energy Stock Balance Sheet, Climate Targets, CCS, DAC, LCA Emission Factors, LCA Energy Consumption Factors

1. INTRODUCTION

Due to the following developments, humankind's energy requirements, including energy bound in food, will continue to rise sharply despite all efforts to increase energy efficiency and save energy:

First, the expected growth of the global population to almost 9.8 billion people by the middle of the century (2054) [1] and the rapid technological development, particularly in the areas of digitalization and artificial intelligence, will lead to an increase in energy and food demand.

Growing living standards and demand for more comfort will lead to larger living and usable spaces per person and thus to a further increase in land sealing which reduces the amount of land available for growing food and energy crops as well as commercial forest and biodiversity areas, which also act as greenhouse gas sinks. The same applies to the expected increase in traffic. Furthermore, the growth of "photovoltaic land sealing" makes it difficult or impossible to cultivate crops on the respective soil or use it as grazing land. Finally, climate change and other factors are leading to an increasing erosion of fertile soils and to decreasing crop yields. As a consequence, the biocapacity of the planet will continue to decline. [2], [3], [4]

The inevitable shift towards renewables requires the energy-intensive development and construction of a global renewable energy generation, storage, and transport infrastructure.

According to IPCC's Special Report 15, net zero by mid of the century cannot be acieved without energy-intensive Carbon Capture and Storage (CCS) and Direct Air Capture (DAC), especially Direct Air Carbon Capture and Storage (DACCS) [5].

Therefore, comprehensive information about the stock of fossil and renewable energy sources available worldwide for use by humankind at a certain point in time, complying with the goal of net zero, is essential in order to identify emerging shortages immediately.

2. CRITICAL ANALYSIS OF EXISTING SYSTEMS

In principle, Environmental-Economic Accounting Systems already comprehensively record the interactions between economic activities and the environment, including mineral resources and land [6].

The Framework of the System of Environmental-Economic Accounting (SEEA), which was adopted as an international standard by the United Nations Statistical Commission, is a multipurpose conceptual framework for understanding the interactions between the economy and the environment, and for describing stocks and changes in stocks of environmental assets. As an accounting system, it enables the organization of information into tables and accounts in an integrated and conceptually coherent manner. [7]

Energy accounts data – including primary energy resources and secondary energy products – are compiled by converting physical measures of mass and volume such as tons, liters and cubic meters into a common unit representing energy content in net calorific terms. The use of the joule as a common measurement unit is recommended by the International Recommendations for Energy Statistics (IRES). [8]

A typical asset account for mineral and energy resources is defined as follows: The accounting year starts with the opening stock, before different additions (such as discoveries, upward reappraisals and reclassifications) and reductions (such as extractions, catastrophic losses, downward reappraisals and reclassifications) in stock are recorded throughout the year, resulting in the closing stock of mineral and energy resources at the end of the year [9]. However, asset accounts for renewable energies are not provided because in the accounting sense of the SEEA Central Framework and SEEA Energy, a physical stock of renewable sources of energy does not exist [10].

Usability of the fossil fuels recorded in the systems of environmental economic accounting, as well as all other energy sources requires not only primary energy resources but also appropriate primary energy extraction and conversion facilities. A prudent assessment can therefore only be ensured by determining and applying the minimum from the capacity-bottleneck of energy extraction and conversion facilities over their average remaining useful life or the resource bottleneck.

As a subsystem of the SEEA Central Framework, SEEA-Energy elaborates in greater detail the links between energy accounts and energy statistics and balances, as described in IRES, and to serve as a bridge between the statistical and energy communities. IRES contribute valuable inputs into the production of tables and accounts of SEEA-Energy, particularly support the use of harmonized definitions of energy products in accordance with the Standard International Energy Product Classification (SIEC) and offer guidance regarding data sources and data compilation. [11]

Furthermore, the SEEA classification of land use consists of the categories: agriculture, forestry, land used for aquaculture, use of built-up and related areas, land used for maintenance and restoration of environmental functions as well as other uses of land not elsewhere classified and land not in use [12].

Energy from natural inputs by type – according to a rough classification in SEEA-Energy – are: Mineral and energy resources (oil, natural gas, coal and peat, uranium and other nuclear fuels), natural timber resources, inputs of energy from renewable sources (solar, wind, wave and tidal, geothermal, other electricity and heat), other natural inputs and energy inputs to cultivated biomass [13].

Energy statistics and energy balances are also the main sources of data for the calculation of energy-related greenhouse gas (GHG) emissions, as the IPCC Guidelines are based on the same conceptual framework. They

address emissions of direct and indirect GHGs. The direct GHGs covered by the guidelines are carbon dioxide (CO_2), methane (CH_4), nitrous oxide (N_2O), hydrofluorocarbons (HFCs), perfluorocarbons (PFCs), sulphur hexafluoride (SF_6) and some others. The indirect GHGs considered in the guidelines are nitrogen oxides (NO_X), ammonia (NH_3), non-methane volatile organic compounds (NMVOC), carbon monoxide (CO) and sulphur dioxide (SO_2). [14]

Traditional energy balances in the sense of energy economics document the generation, conversion, and use of energy sources in a national economy comprehensively, detailed (by sector) and consistent in the form of a matrix [15]. Based on classical energy balances, energy flow diagrams are created that visualize the process of energy conversion from primary energy to useful energy, including energy losses [16]. An energy balance is therefore a calculation of energy flows over a period of time and not a representation of energy resources at a given point in time.

The critical analysis of existing systems can therefore be summarized as follows:

First of all, the existing systems pursue different goals. They do not reflect the requirement for prudent, bottleneck-oriented, and point-in-time-related recording of all energy stocks – including renewables – and they do not take into account energy consumption for CCS and DACCS.

Nevertheless, it makes sense to base the balance sheet items of the WESBS on the standardized terminology of the existing systems, which also enables comprehensive data compatibility. SEEA Central Framework and SEEA-Energy provide the conceptual basis and terminology for a range of asset data on fossil energy resources as well as land and marine-based biocapacity.

Even though SEEA is primarily a concept for establishing national systems of Environmental-Economic accounting, the terminology can also be used for a WESBS. Finally, the statistical data on energy conversion losses recorded in classical energy balances can contribute to the dimensioning of provisions for energy conversion losses (see below) in the WESBS.

3. CONCEPTIONAL BASICS OF A WORLD ENERGY STOCK BALANCE SHEET

The World Energy Stock Balance Sheet (WESBS) is a system for presenting global energy assets at a specific point in time, applying the principle of prudence borrowed from business accounting. WESBS also takes into account the energy consumption in the form of provisions (liabilities of uncertain timing or amount) that will be incurred for CCS and DACCS.

The assets side of the global energy stock balance sheet shows all fossil and renewable primary, secondary, and final energy stocks prudently valued in PJ at the balance sheet date. Primary energy resources are in accordance with the terminology of SEEA-Energy (see above): mineral and energy resources (oil, natural gas, coal and peat, uranium and other nuclear fuels), natural timber resources, renewable sources (solar, wind, wave tidal, geothermal, etc.), other natural inputs and cultivated biomass. Additionally, potential crop yields for food production, livestock suitable for consumption and unprotected wild animal and fish stocks are also primary energy resources capitalized on the assets side of the WESBS.

In accordance with the principle of prudence, either the primary energy extraction and conversion facilities capacity bottleneck over its remaining useful life or the resources bottleneck – each valued of course in PJ – represents the upper valuation limit of the respective energy source on the assets side. Facilities in the sense of the WESBS include e.g. gas/oil drilling rigs/equipment on land or sea, mining equipment, refineries, coal, oil, nuclear, solar, wind, geothermal, tidal and hydroelectric power plants, combined heat and power plants (CHPs), as well as sufficient harvesting equipment available at harvest times, fishing/hunting equipment and slaughterhouse capacity.

The bottleneck-oriented valuation in the WESBS – demonstrated by using the example of renewable primary energy assets (e.g., solar energy for photovoltaic electricity generation) – should be generally carried out as follows:

Because solar energy can be effectively considered as unlimited, the bottleneck is on the side of all photovoltaic systems installed worldwide and their ability to convert solar inputs into electricity over their expected remaining useful life. At the balance sheet date, the primary energy source solar energy for power generation is therefore recognized in the WESBS as the cumulative expected solar input in PJ over the expected remaining useful life of all photovoltaic systems installed worldwide.

Specifically, the assessment of solar energy as a primary energy source for photovoltaic power generation is calculated by multiplying the expected remaining useful life of all photovoltaic systems installed worldwide in years by the cumulative expected solar input into all photovoltaic systems installed worldwide in PJ per year. All expected values could be determined on the basis of statistical averages in the past, unless the latest findings on the balance sheet date of the WESBS indicate a higher or lower value.

Furthermore, independently from the example of solar energy for photovoltaic power generation, it could be discussed for all primary energy sources whether energy extraction and conversion facilities that have already been planned and approved but are not yet in operations should also be included in the bottleneck-oriented assessment. In this case, appropriate provisions (see below for details) for the energy consumption that will still be incurred until they are commissioned, as well as the energy consumption for neutralizing the CO_2e that will still be incurred until commissioning by CCS and DACCS would have to be recorded on the liabilities side of the WESBS. However, a strict interpretation of the principle of prudence would favor a restriction to plants that are already commissioned at the balance sheet date, especially since political, legal and economic risks could lead to a temporary or permanent construction freeze.

Furthermore, the assets side includes all fossil and renewable energy and food products in PJ that are still within the energy conversion sector on the balance sheet date as secondary energy sources. These are energy products that are in interim storages or on their way to the end consumer on the balance sheet date, e.g. heating oil, gasoline and gas stocks, nuclear fuel elements, briquettes, coking coal, waste intended for incineration in waste incineration plants, firewood, electricity stored in battery storages and food products of all kinds.

Finally, all fossil and renewable final energy and food products that are already directly available to end energy consumers for conversion into useful energy are recorded on the assets side in PJ.

Facility and equipment bottlenecks – such as an insufficient number of battery storages for renewable electricity leading to energy losses – that occur on the way from activated secondary and final energy sources to the energy consumer do not reduce their asset value in the WESBS, but are recorded as provisions for energy losses.

The liabilities side includes provisions for all estimated energy consumption and losses in PJ that are expected to arise during the conversion of capitalized primary, secondary, and final energy stocks into useful energy. This also includes the energy consumed by food production and distribution, as well as energy losses due to food waste that occur on the way from farming, livestock breeding, hunting and fishing to consumption.

In addition, liabilities have to be recognized for the energy consumption by CCS and DACCS to neutralize GHG emissions arising during conversion/use of the capitalized energy sources. Finally, a DACCS provision must also be recorded for atmospheric CO_2e, as soon as and as far as the CO_2e budget limitation in the atmosphere – intended to achieve the 1.5°C target with overwhelming probability – will be exceeded in the future.

The energy consumption for CCS and DACCS to ensure net zero is calculated using emission factors followed by the calculation of the energy consumption for CCS and DACCS. As far as facilities for CCS and DACCS do not exist on the balance sheet date, their construction consumes energy and, depending on the energy sources used, also generates CO_2-e, emissions. In this case, emission factors and energy consumption factors must be determined on the basis of a life cycle assessment (LCA).

However, already on the balance sheet date existing extraction, conversion, transport, storage, CCS, and DACCS infrastructures may not be included in the WESBS as provisions using LCA emission factors and LCA energy consumption factors, as the energy required to construct these infrastructures has already been consumed and is therefore no longer included in the energy assets. The same applies to the GHGs already emitted as a result of the construction of these infrastructures. Those emissions are already in the atmosphere on the balance sheet date and could lead to DACCS liabilities for atmospheric CO_2e above 1.5°C – perhaps in the nearest future – if the conditions described above are met.

The difference between energy assets and energy liabilities results in energy equity, which is available, if the 1.5°C target is met. Energy equity thus represents the net energy assets or "useful energy capital" of humankind at a given point in time. An aggregated WESBS could look like this:

Energy Assets	**WESBS at Dec. 31st 2027 in PJ**	**Energy Liabilities**
Primary Energy (PE), fossil and renewable		Provisions for energy losses from PE to Useful Energy (UE) Provisions for CCS/DACCS from PE to UE
Secondary Energy (SE), fossil and renewable		Provisions for energy losses from SE to UE Provisions for CCS/DACCS from SE to UE
Final Energy (FE), fossil and renewable		Provisions for energy losses from FE to UE Provisions for CCS/DACCS from FE to UE
		DACCS Liabilities for atmospheric CO_2e above 1.5°C
		Energy Equity
Balance Sheet Total Assets		**Balance Sheet Total Liabilities**

Overall, the following applies:

Energy Assets = Energy Equity + Energy Liabilities (1)

Energy Equity = Energy Assets – Energy Liabilities (2)

Of course, all primary, secondary, and final energy assets, as well as their corresponding provisions, are recorded in sufficient detail and transparency so that the contribution of each energy source or product to the energy equity can be determined.

4. CONCLUSIONS AND NEXT STEPS

In analogy to any business balance sheet, the WESBS could also be subject to an in-depth analysis.

First, it could answer the fundamental question of how long the energy equity determined on the balance sheet date could satisfy humankind's total useful energy demand and how long the useful energy output of a single energy resource (e.g. crop yields, solar energy for photovoltaic power generation, etc.) could satisfy the useful energy demand for this specific energy resource.

Furthermore, energy efficiency indicators could be determined at different levels as the relationship between energy input and useful energy output. Therefore, global energy efficiency can be calculated like:

Global Energy Efficiency = Energy Equity / Global Energy Assets (3)

Improvements in global energy efficiency – such as progress in energy saving technology or a shift to primary energy resources with a higher energy efficiency – will lead ceteris paribus to an increase in energy equity. For example, the efficiency for certain prime energy resources can be determined as follows:

Example 1: Fossil energy assets (e.g., hard coal for power generation):

$\text{Energy Efficiency}_{\text{Hard\_Coal}} = \text{Useful Energy}_{\text{Hard\_Coal}} / \text{Primary Energy Assets}_{\text{Hard\_Coal}}$ (4)

Example 2: Renewable energy assets (e.g., photovoltaics for power generation):

$\text{Energy Efficiency}_{\text{Photovoltaics}} = \text{Useful Energy}_{\text{Photovoltaics}} / \text{Primary Energy Assets}_{\text{Photovoltaics}}$ (5)

However, the next major challenge will be to quantify the balance sheet items. LLM-based approaches are currently being tested with ChatGPT to find relevant and up-to-date scientific studies to ensure a reliable quantification process.

In the future, it would be interesting to develop national energy stock balance sheets (NESBS) to reach the goals of a WESBS also on a national level. A consolidated aggregation of all national NESBS together with the rest of the world's energy assets and liabilities to a global WESBS could create a consistent information system about energy stocks on national, supra-national (e.g. EU) and global levels.

Furthermore, the WESBS could also serve as a starting point for simulations. For example, the macroeconomic and global effects of technological progress in terms of higher CO_2e and energy efficiency on the growth of energy equity could be simulated.

Finally, the WESBS could also contribute to the vision that energy consumption will no longer be included in the gross national product and thus no longer contributes to economic growth. Rather, the development of energy equity over time could be a significant indicator of sustainable growth.

ACKNOWLEDGMENT

Special thanks to the free version of DeepL, which was used to refine style and grammar. All final edits and decisions were made exclusively by the author [17].

REFERENCES

[1]. United Nations, *World Population Prospects 2024: Summary of Results*, UN DESA/POP/2024/TR/NO. 9, p. 53, Department of Economic and Social Affairs, New York, 2024.

[2]. M. A. Moros-Ochoa, G. Y. Castro-Nieto, A. Quintero-Español, C. Llorente-Portillo, "Forecasting Biocapacity and Ecological Footprint at a Worldwide Level to 2030 Using Neural Networks", *Sustainability 2022*, 14, 10691, https://doi.org/10.3390/su141710691.

[3]. E. J. Molina Bacca, M. Stevanovic, B. L. Bodirsky, J. C. Doelman, L. Parsons Chini, J. Volkholz, K. Frieler, C. P. O. Reyer, G. Hurtt, F. Humpenöder, K. Karstens, J. Heinke, C. Müller, J. P. Dietrich, H. Lotze-Campen, E. Stehfest, A. Popp, "Future land-use pattern projections and their differences within the ISIMIP3b framework", *Earth System Dynamics*, 16, 753–801, 2025, https://doi.org/10.5194/esd-16-753-2025.

[4]. J. Braun, C. Werner, D. Gerten, F. Stenzel, S. Schaphoff, W. Lucht, "Multiple planetary boundaries preclude biomass crops for carbon capture and storage outside of agricultural areas", *Communications Earth & Environment*, 2025, 6:102, https://doi.org/10.1038/s43247-025-02033-6.
[5]. IPCC, Special Report 15, *Global warming of 1,5 °C*, p. 15 - 17, 2019.
[6]. U. Scherhag, *System of Environmental Economic Accounting – Energy Accounting*, p. 6 - 8, German Federal Statistical Office, DESTATIS, Wiesbaden, 2022.
[7]. United Nations, *System of Environmental-Economic Accounting 2012 – Central Framework*, Preface, p. vii - p. viii, New York, 2014.
[8]. United Nations, *System of Environmental-Economic Accounting 2012 – Central Framework*, p. 60, New York, 2014.
[9]. United Nations, *SEEA-Energy – System of Environmental-Economic Accounting for Energy*, p. 96, Department of Economic and Social Affairs, Statistics Division, New York 2019.
[10]. United Nations, *System of Environmental-Economic Accounting 2012 – Central Framework*, p. 172, New York, 2014.
[11]. United Nations, *SEEA-Energy – System of Environmental-Economic Accounting for Energy*, Preface 2019, p. iii and p. 11, Department of Economic and Social Affairs, Statistics Division, New York 2019.
[12]. United Nations, *System of Environmental-Economic Accounting 2012 – Central Framework*, p. 175, New York, 2014.
[13]. United Nations, *SEEA-Energy – System of Environmental-Economic Accounting for Energy*, p. 32, Table 2.5, New York, 2019.
[14]. United Nations, *International Recommendations for Energy Statistics*, p. 141 - 142, Department of Economic and Social Affairs, New York, 2019.
[15]. H. G. Buttermann, T. Baten, T. Nieder, *Further development of the model for an early estimation of the energy balance*, p. 25, German Working Group on Energy Balances (AGEB e.V.), Ed.: German Environment Agency, Dessau-Rosslau, 2024.
[16]. AGEB, bdew, FfE, HEA, Interactive Energy flow diagram for the Federal Republic of Germany 2023, bdew website. [Online]. Available: https://www.bdew.de/media/documents/3_Energieflussbild_Deutschland_2023_PJ_detailliert.svg
[17]. Based on a recommendation from ChatGPT to acknowledge the use of DeepL in this context (Question for and response from ChatGPT on Sept. 27, 2025, 23:26 CEST).

EJSDR
European Journal of Sustainable Development Research
e-ISSN : 2458-8091

Enhancing Thermal Efficiency of Panel Radiators Through Turbulence-Inducing Modifications in Water Channels

Umut Ucak[1]*, Cisil Timuralp[2]

[1] *Türk Demirdöküm Factory Inc. R&D department, Bozüyük / Türkiye*

[2] *Eskisehir Osmangazi University, Faculty of Engineering, Department of Mechanical Engineering, Eskisehir / Turkey.*

**Corresponding Author email: umut.ucak@vaillant-group.com*

Abstract

This study aims to improve the thermal efficiency of panel radiators, which are widely used in building heating systems. By promoting turbulent flow inside the water channels, heat transfer can be increased without raising energy use. In the modified design, small 90° rectangular blocks (5 mm wide and 10 mm long) are added inside the vertical channels to create turbulence. This design distinguishes itself from other methods by creating turbulence through indentations in the sheet metal that forms the channel, rather than using additional turbulators such as twisted tape inserts or wire coil inserts. This unique strategy not only boosts heat transfer performance but also leads to energy savings, reduced emissions, and more efficient heating in both residential and commercial buildings. With the modified design, due to increased friction, the pressure rise shows a 1.36% increase compared to the current design. Meanwhile, the temperature of the water circulating in the panel radiator channels has decreased further compared to the current design, resulting in a 1.21% increase in ΔT. This indicates that the modified design transfers more heat from the water to the environment, causing the water's outlet temperature to drop more significantly. Additionally, with the modified design, the water contact surface area has decreased by 0.64 m², while the water heat flux has increased by approximately 25% compared to the current design. The higher heat flux achieved with a smaller water contact surface area demonstrates the efficiency of the system compared to the existing design.

Key words

Energy Efficiency, Heat Transfer Enhancement, Panel Radiator, Turbulent Flow

1. INTRODUCTION

In the context of modern energy policies, energy efficiency is regarded as a critical parameter for both sustainable economic development and environmental protection [1]. Enhancing the thermal efficiency of panel radiators, which are widely utilized in building heating systems, directly contributes to reducing energy demand in the residential and commercial sectors. High-efficiency radiator designs can deliver the required thermal output with lower energy input, thus minimizing fossil fuel consumption, decreasing operational costs, and improving national energy security by reducing dependency on external energy sources. Moreover, the reduction in energy consumption results in lower greenhouse gas emissions, thereby contributing to climate change mitigation and global sustainability goals [2]. Recent industrial studies emphasize that technological advancements in panel radiator manufacturing processes play a key role in improving both product quality and energy efficiency. Modern

production techniques such as high-tonnage pressing, multi-point spot welding of convector sheets, and optimized surface treatments significantly enhance heat transfer performance while reducing manufacturing defects and material waste [3]. From a thermal engineering perspective, the enhancement of convective heat transfer can be achieved through various flow and surface modification strategies. Among these, promoting turbulent flow is particularly effective. In contrast to laminar flow characterized by orderly fluid layers turbulent flow involves chaotic motion, eddies, and vortices, which reduce the thermal boundary layer thickness at the fluid–solid interface and significantly increase the convective heat transfer coefficient [4]. To this end, surface optimization through methods such as increasing roughness, implementing extended surfaces (fins), introducing swirl flow, and applying turbulence-enhancing geometrical modifications are frequently employed in heat transfer enhancement studies. The analysis results provide essential insights for radiator design optimization, offering practical contributions toward improving thermal performance, reducing energy consumption, and minimizing environmental impact in heating applications.

2. MATERIALS AND METHODS

In the literature, various turbulent flows contribute positively to thermal efficiency. In the study by Pour Razzaghi et al. numerical analyses on turbulent fluid flow and heat transfer in twisted flat tubes are presented. In the research, three different geometries for the cross-section of the flat tube were examined, and water with constant thermophysical properties was used as the working fluid. The Reynolds number ranges from 5000 to 20000. The results show that twisted flat tubes increase efficiency by nearly 70% compared to smooth tubes with the same surface area and hydraulic diameter. Additionally, the alternating helical direction increases efficiency by almost 60%, which is noted as a good choice. Due to the effect of helical pitch on the flow path, the alternating geometry performed better at some Reynolds numbers. These results are explained using characteristic flow contours such as turbulent kinetic energy, tangential velocity, and temperature. The results are presented in numbers and plots for a more accurate comparison [5]. In another study conducted by R. Yang and F. P. Chiang, experiments were conducted using water as the working medium, flowing through a varying-curvature curved pipe, forming a double-pipe heat exchanger. The heat transfer coefficients were determined using the Wilson plot method. The effects of Dean, Prandtl, Reynolds numbers, and curvature ratio on heat transfer and friction factors were examined. The results showed that a higher Dean number leads to a higher heat transfer rate. Compared to a straight pipe, the heat transfer rate can be increased by up to 100%, while the friction coefficient increased by less than 40%. These findings suggest that using S-shaped pipes instead of straight pipes could be advantageous for performance enhancement in heat exchangers, such as solar collectors [6]. A separate investigation by A. Lanani and R. Benchabi explores the two-dimensional heat transfer characteristics within a corrugated channel. Heat exchangers are vital in energy management across various industries, designed to maximize heat transfer through specialized surfaces. Techniques like corrugated surfaces enhance turbulence and heat transfer. A study using Fluent CFD code explores the impact of Reynolds numbers on flow and heat transfer, revealing that friction and Nusselt numbers are affected by Reynolds numbers and outperform those in smooth channels [7]. The study conducted by Soorena Azarhazin et al. it was found that utilizing different pipe geometries, specifically flattened pipes, increases turbulence and unsteadiness, making them promising candidates for thermal applications due to enhanced heat transfer coefficients [8].

Within the scope of these studies, the primary objective is to enhance the thermal performance of panel radiators by promoting turbulent flow through controlled friction augmentation, achieved via specially designed geometric modifications within the vertical water channels. Figure 1-a presents the reference radiator configuration featuring straight vertical channels, which inherently promote predominantly laminar or transitional flow regimes. In contrast, Figure 1-b illustrates the modified radiator design incorporating 90° rectangular constrictions (5 mm in width and 10 mm in length) periodically integrated into the channel walls. Unlike conventional heat transfer enhancement techniques that rely on additional turbulence promoters such as twisted tape inserts, wire coils, or internal fins, the proposed approach induces turbulence directly through localized geometric deformation of the sheet metal forming the channel. This method offers a distinct advantage by eliminating the need for extra components, thereby avoiding additional material usage, assembly complexity, and potential flow blockages. Moreover, since the indentations are formed during the standard pressing process, the solution maintains full compatibility with mass production techniques and does not introduce extra manufacturing steps or costs.

As illustrated in Figure 2, the side view of the existing radiator with a straight water channel, the corresponding view of the newly developed indented channel model, and the detailed geometry of the indentation form are presented. The cross-sectional analysis reveals the precise structural configuration of the modified channel. While the overall channel width is preserved at 12 mm to maintain hydraulic compatibility with existing systems, stepped indentations of 5 mm depth are symmetrically introduced on both side walls, separated by a 10 mm vertical flat segment. This alternating stepped geometry generates periodic contractions and expansions along the flow path. From a fluid dynamics perspective, these abrupt geometric variations act as flow disruptors, inducing local acceleration, deceleration, and separation zones. As a result, recirculation regions, vortical structures, and secondary flow patterns are formed downstream of each indentation. These phenomena significantly intensify turbulence levels, leading to repeated thinning and redevelopment of the thermal boundary layer along the channel walls. Consequently, the convective heat transfer coefficient is enhanced due to increased momentum and thermal mixing within the fluid core. Furthermore, the modified geometry increases the wetted perimeter, effectively enlarging the active heat transfer surface area despite maintaining the same nominal channel width. More importantly, the complex internal surface topology promotes chaotic fluid motion, which enhances radial mixing and disrupts temperature stratification inside the channel. This results in a more uniform temperature distribution across the cross-section and improves overall thermal energy extraction from the flowing water.

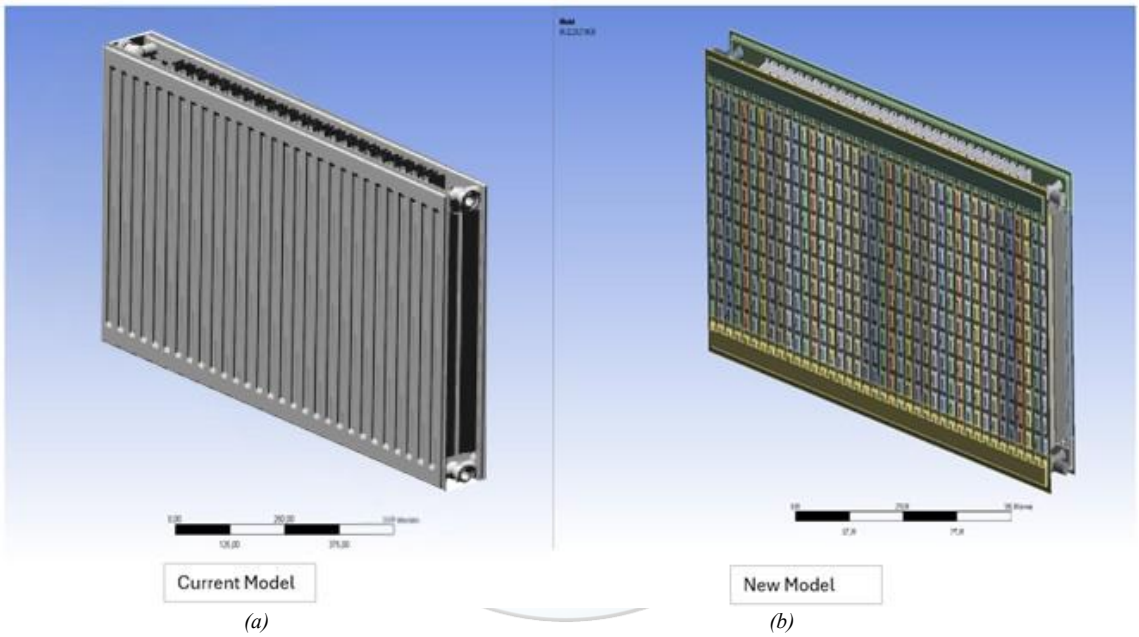

Figure 1. (a) Radiator with existing water channel, (b) Radiator with indented water channel [9]

In addition to thermal benefits, the stepped indentations introduce a moderate increase in flow resistance, causing a controlled pressure drop that is indicative of enhanced turbulence intensity. However, this hydraulic penalty remains within acceptable operational limits, ensuring that the overall thermo-hydraulic performance remains favorable. Therefore, the proposed geometry achieves an optimal balance between heat transfer enhancement and pressure loss, making it a highly efficient and industrially viable solution for next-generation panel radiator designs.

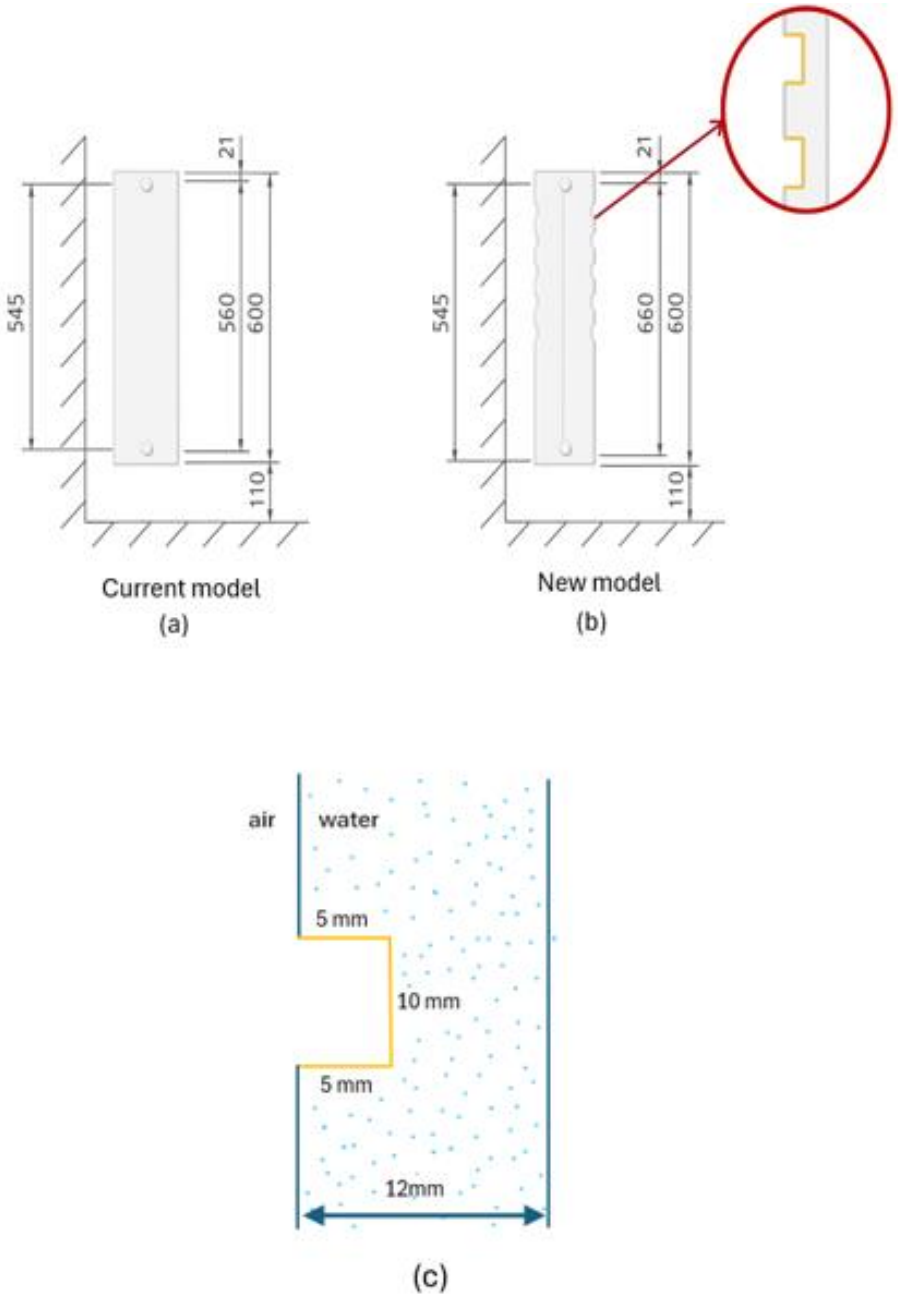

Figure 2. (a) Side view of radiator with existing water channel, (b) Side view of radiator with indented water channel, (c) dimensions of the indentation form [10]

Flow analyses were performed using Ansys Fluent 18.02 to assess the heat transfer efficiency of both designs. In the analysis settings, the viscous model for the current design is set to laminar, while the modified design employs the k-ε realizable model with non-equilibrium wall functions, offering a more sophisticated method for capturing turbulent flow characteristics. The k-ε realizable model was chosen for its ability to provide more accurate predictions of turbulent flow behavior, especially in complex geometries and high Reynolds number flows [11]. Furthermore, the material properties used in the analysis are detailed in Table 1.

Table 1. Properties of materials

Part	Material	Density (kg/m³)	Specific Heat (J/kg·K)	Thermal Conductivity (W/m·K)	Viscosity (kg/m·s)
Fluid	Water	977.78	4189.5	0.6663	0.000404
Panel	DC01	7870	505	5.4	-
Convector	DC01	7870	505	5.4	-
Elbow	DC01	7870	505	5.4	-

In this analysis, the performance and heat transfer of a radiator were examined. The water inlet and outlet connections of the radiator are important factors that affect the direction of water flow and consequently the heat transfer. In this scenario, the water inlet is provided from the top and the outlet from the bottom. The water flow is maintained at a rate of 0.0103 kg/s, and the water temperature is assumed to be 75 ℃. It was chosen this way based on the assumption that the heat transfer efficiency would be higher in cross-flow. This temperature is sufficient to ensure effective heat dissipation by the radiator. As the water circulates within the radiator, it transfers heat to the air across the surface area. The air flow is modeled as natural flow, with an initial temperature set at 20 ℃. Natural air flow refers to the movement of air caused by temperature differences, without the use of any fan or pump.

This type of flow generally occurs at lower speeds, and therefore, the heat transfer may be more limited compared to air flow. During the analysis, as illustrated in Figure 3 a mesh with approximately 30 million elements was created for the radiator and the surrounding flow area. This high-resolution mesh allows for more precise and accurate results in fluid dynamics simulations. The average mesh size was determined to be 0.25, indicating a rather fine mesh structure, which is a suitable choice for detailed analysis. This detailed mesh structure enables better modeling of the movement of water within the radiator, air flow, and heat transfer. The quality and size of the mesh are factors that directly affect the accuracy of the simulation. Therefore, the mesh structure used in this analysis is critically important for accurately evaluating the performance and heat transfer of the radiator.

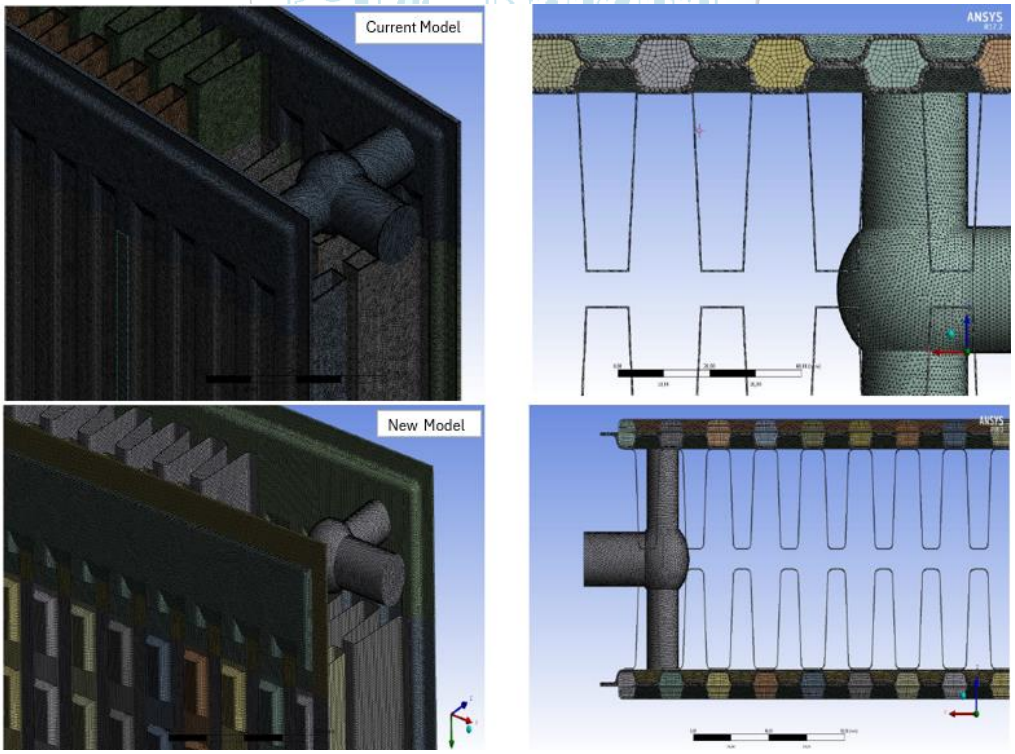

Figure 3. Mesh structure

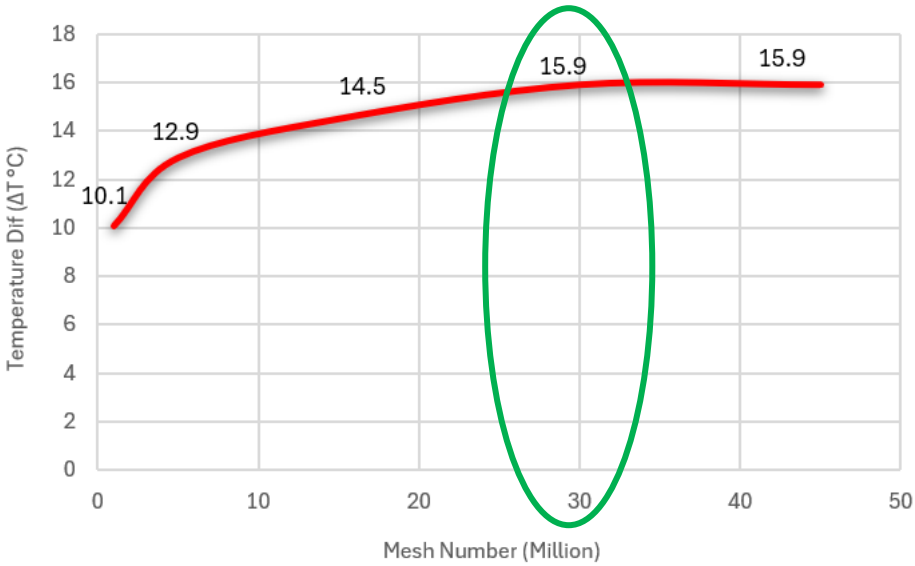

Figure 4. Results of independence from Mesh

As observed in Figure 4, increasing the number of mesh elements does not lead to significant variation in the results, confirming that the selected mesh configuration is independent of grid size. This validates the numerical stability and reliability of the CFD simulations performed in this study.

3. RESULT AND DISCUSSION

In order to compare the thermal and hydraulic performances of the current and modified radiator designs, cross-sectional data were extracted from three different planes along the flow direction. These planes were selected to capture the local variations in velocity, pressure, and temperature fields induced by the geometric modifications. Figure 5 presents the temperature contour distributions obtained under identical boundary conditions for both designs. As clearly observed in Figure 5, the modified radiator design exhibits a significantly enhanced heat transfer performance compared to the baseline configuration. The blue-colored regions, representing lower temperature zones (cold regions), are substantially reduced in the modified design. This indicates that a larger portion of thermal energy is transferred from the circulating water to the surrounding air. The temperature field in the modified geometry is more uniformly distributed, confirming the effectiveness of turbulence generation in promoting thermal mixing.

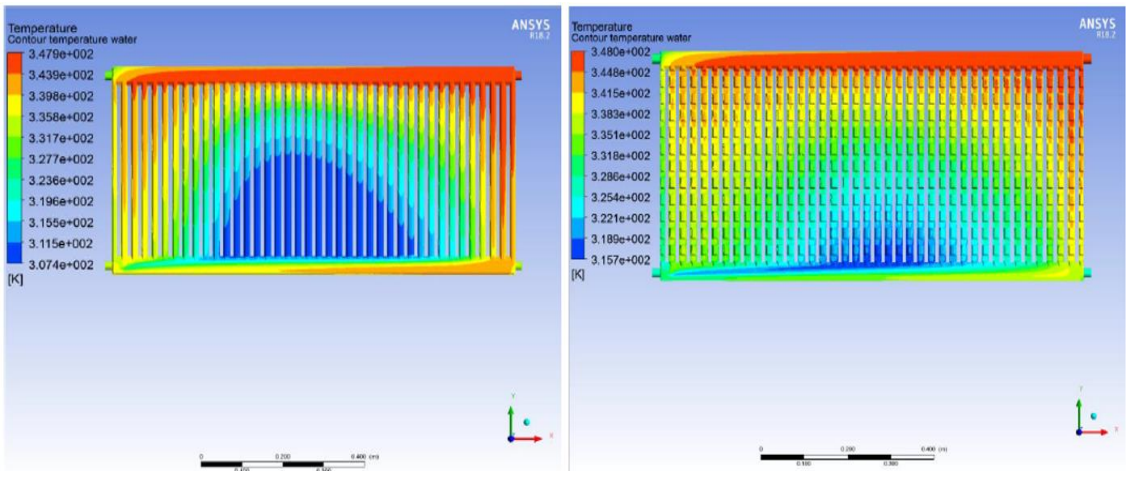

(a) *(b)*

Figure 5. Temperature distributions (a) Current design, (b) Modified design

The quantitative results summarized in Table 2 further support these observations. Although the wetted surface area in the modified design slightly decreases from 1.8171 m² to 1.8055 m² (approximately 0.64% reduction), the average wall heat flux increases remarkably from 384.56 W/m² to 480.38 W/m², corresponding to an enhancement of nearly 25%. This clearly demonstrates that the dominant mechanism governing heat transfer improvement is turbulence intensity rather than surface area enlargement. The periodic indentations continuously disrupt the thermal boundary layer, allowing higher temperature gradients at the wall-fluid interface, which directly increases convective heat transfer rates. Moreover, the outlet water temperature in the modified radiator decreases from 332.1 K to 327.9 K, resulting in a temperature difference of 4.2°C compared to the reference design. This temperature drop (ΔT) indicates that more thermal energy is extracted from the working fluid along the flow path. Such a behavior is a direct consequence of enhanced mixing and increased residence time of fluid particles near the heated walls due to recirculation zones formed downstream of each indentation.

Table 2. Analysis Outcomes

Design	Input pressure (Pa)	Output pressure (Pa)	Input temperature (K)	Output temperature (K)	Water contact surface area (m^2)	Water heat flux (W/m^2)
Current	5.9	0.6	348	332.1	1.8171	384.562
Modified	5.9	0.68	348	327.9	1.8055	480.383

The pressure drop across the radiator slightly increases from 0.6 Pa to 0.68 Pa, corresponding to a marginal rise of approximately 1.36%. This increase is attributed to additional friction losses and form drag caused by the stepped indentations. However, when evaluated in terms of overall thermo-hydraulic performance, this pressure penalty is negligible compared to the significant heat transfer enhancement obtained. This confirms that the proposed geometry achieves a highly favorable trade-off between thermal gain and pumping power requirement. These flow structures increase turbulent kinetic energy and promote strong momentum exchange between the near-wall region and the core flow. Consequently, the hydrodynamic and thermal boundary layers are repeatedly disrupted, which prevents boundary layer thickening and sustains high heat transfer coefficients throughout the channel length. In addition, the modified geometry suppresses temperature stratification across the channel cross-section. In the baseline design, the temperature gradient between the core flow and near-wall regions is more pronounced, indicating weaker mixing. In contrast, the modified design exhibits a more homogeneous temperature distribution, proving the effectiveness of geometrical turbulence generation.

Overall, these findings are consistent with previous studies reported in the literature [5–8], where enhanced turbulence through geometric modifications led to significant improvements in heat transfer performance.

CONCLUSIONS

This study numerically investigated the thermal and hydraulic performance of a panel radiator featuring turbulence-inducing geometrical modifications within its vertical water channels. Based on comprehensive CFD analyses, the following conclusions are drawn:

- The integration of 90° rectangular indentations (5 mm width, 10 mm length) successfully transformed the internal flow regime from laminar to turbulent, leading to a pronounced enhancement in convective heat transfer.
- Despite a slight reduction in wetted surface area (1.8171 m² to 1.8055 m²), the modified design achieved a ~25% increase in heat flux, clearly demonstrating that turbulence intensity has a more dominant influence on thermal performance than surface area alone.
- The outlet water temperature of the modified radiator decreased by 4.2 °C compared to the baseline configuration, indicating a higher thermal energy extraction from the working fluid.
- The increased temperature drop (ΔT) across the radiator confirms the superior heat transfer capability of the proposed geometry.
- A marginal pressure rise of 1.36% was observed due to increased friction effects. However, this hydraulic penalty is negligible when compared to the substantial thermal performance improvement, confirming a favorable thermo-hydraulic trade-off.
- Temperature contour visualizations revealed a significant reduction in low-temperature zones, indicating more uniform heat distribution across the radiator surface.
- The k-ε Realizable turbulence model combined with non-equilibrium wall functions proved effective in capturing complex flow structures induced by the geometric modifications.
- Unlike conventional enhancement techniques employing additional turbulators (e.g., twisted tapes, wire coils), the proposed method achieves turbulence solely through channel geometry modification, offering key industrial advantages:
    - ✓ No additional components
    - ✓ Zero material cost increase
    - ✓ High manufacturing compatibility
    - ✓ Improved structural integrity
    - ✓ Scalability for mass production
- From an energy efficiency standpoint, the enhanced thermal performance enables:
    - ✓ Lower supply water temperatures
    - ✓ Reduced boiler load
    - ✓ Shorter heating response times
    - ✓ Decreased fuel consumption
    - ✓ Lower greenhouse gas emissions
- The obtained results show strong agreement with previous studies on turbulence-enhanced heat transfer, validating the scientific reliability of the present work.

.

ACKNOWLEDGMENT

Turk Demirdokum Fabrikaları A.Ş. is acknowledged for their valuable contributions.

CONFLICT OF INTEREST STATEMENT

The authors declare no conflicts of interest regarding this manuscript.

REFERENCES

[1]. X. Chavanne (Ed.), Energy Efficiency: What It Is, Why It Is Important, and How to Assess It (Energy Science, Engineering and Technology), Nova Science Publishers Inc., New York, 2013, pp. 120, ISBN: 9781628087642.
[2]. A. Çağlar, "Effects of using BN/water nanofluid on the thermal performance, energy saving, and power consumption of a panel radiator heating system," Case Studies in Thermal Engineering, 2025, doi: https://doi.org/10.1016/j.csite.2025.106024
[3]. U. Uçak, Ç. Timuralp, and T. Amcaoğlu, "Panel radyatör ve üretim prosesinin araştırılması," Mühendis ve Makina / Engineer and Machinery, vol. 66, no. 719, pp. 313–330, 2025, doi: https://doi.org/10.46399/muhendismakina.1727135
[4]. A. Tohidi, S. M. Hosseinalipour, M. Shokrpour, and A. S. Mujumdar, "Heat transfer enhancement utilizing chaotic advection in coiled tube heat exchangers," Applied Thermal Engineering, vol. 76, pp. 185-195, 2015, doi: https://doi.org/10.1016/j.applthermaleng.2014.10.073
[5]. M. J. Pour Razzaghi, M. Ghassabian, M. Daemiashkezari, A. N. Abdulfattah, H. Hassanzadeh Afrouzi, and H. Ahmad, "Thermo-hydraulic performance evaluation of turbulent flow and heat transfer in a twisted flat tube: A CFD approach," Case Studies in Thermal Engineering, vol. 35, 2022, doi: https://doi.org/10.1016/j.csite.2022.102107.
[6]. R. Yang and F. P. Chiang, "An experimental heat transfer study for periodically varying-curvature curved-pipe," Int. J. Heat Mass Transf., vol. 45, pp. 3199-3204, 2002.
[7]. A. Lanani and R. Benchabi, "Two-Dimensional Study of Heat Transfer Characteristics Flow in a Corrugated Channel," Mechanics of Fluids and Gases, vol. 22, no. 2, 2016, doi: https://doi.org/10.5755/j01.mech.22.2.13321.
[8]. S. Azarhazin, M. Soleimani, J. Kozinski, and A. Tarokh, "The influence of changing pipe cross section on the turbulent flow and heat transfer," International Communications in Heat and Mass Transfer, vol. 166, 2025, doi: https://doi.org/10.1016/j.icheatmasstransfer.2025.109126.
[9]. Ansys Fluent 18.02
[10]. Demirdöküm, (2014). Technical archive
[11]. A. J. Jaworski (Ed.), Selected Problems in Fluid Flow and Heat Transfer, MDPI Books, Basel, Switzerland, 2019, doi: https://doi.org/10.3390/books978-3-03921-428-0

EJSDR
European Journal of Sustainable Development Research
e-ISSN : 2458-8091

Comparative Analysis of Energy Footprints of Traditional and Green Building Materials: Towards the Net Zero Construction Goal

Prof.Dr.Ayşe Arıcı
Intarnational Vision University, Faculty of Engineering and Architecture, Department of civil Engineering, Gostivar, North Macedonia,
**email:aysearici.iut@gmail.com*

Abstract

Globally, the construction sector is one of the most critical industries regarding environmental sustainability due to its high energy consumption and resulting carbon emissions. This study aims to reveal the energy footprint differences between traditional and green building materials, in line with the goal of "net-zero construction," by examining building materials' embodied energy and operational energy components throughout their life cycle, from production to end-of-use.

The research collected data on production, procurement, and application processes through a Likert-type survey administered to 180 construction material manufacturers and suppliers operating in Turkey. The data were evaluated using factor analysis and multivariate regression models, and a life cycle assessment (LCA) was also conducted for three material categories: conventional binders, sustainable alternatives, and hybrid systems.

The results show that green materials consume an average of 28% less total energy during production than conventional systems. Bio-based binders, in particular, reduce maintenance requirements, resulting in long-term energy savings. However, high production costs and limited supply infrastructure slow down the transition to sustainable materials. The research demonstrates that the widespread adoption of green materials depends on technological innovation, policy incentives, standardization, and cross-sector collaboration.

Key words

Green building technologies · Carbon reduction in the construction sector, Structural Reinforcement Systems, Technology, Sustainable Material, Structural Innovation.

1. INTRODUCTION

Globally, the construction sector is at the center of environmental sustainability discussions as one of the industries with the highest energy consumption and carbon emissions. According to data from the International Energy Agency (IEA, 2023), the construction sector is responsible for approximately 36% of global energy use and 39% of total greenhouse gas emissions. This figure includes the energy consumed by buildings during their use and the indirect energy consumption (embodied energy) generated during material production, transportation, application, and post-use disposal. This demonstrates that the environmental impacts of building materials are not limited to their lifespan; energy expenditures throughout the production and supply chain must also be considered (Cabeza et al., 2014). Therefore, the concept of the energy footprint is gaining importance as a fundamental indicator in assessing the environmental performance of the construction sector.

In recent years, "net-zero construction" has become a priority goal in sustainable architecture, engineering, and materials science. This approach aims to balance the energy consumed by a building throughout its lifecycle with renewable energy sources (Dixit, 2019). In other words, converging the balance between a building's energy inputs and outputs to zero necessitates energy efficiency in both production and usage phases. However, achieving this goal is directly related to structural design and energy systems, material selection, production technology, and supply chain management. Material choices constitute one of the most critical parameters determining a building's overall energy performance (Giesekam et al., 2016).

Traditional building materials, particularly Portland cement, steel, aluminum, and reinforced concrete systems, have significant environmental impacts on embodied carbon due to their high-energy-intensive production processes. For example, producing one ton of cement releases approximately 0.9 tons of CO_2, while steel production can release up to 1.8 tons (Hammond & Jones, 2011). These materials' prevalence and rising energy costs make it difficult to reduce carbon emissions and delay net-zero construction targets. Furthermore, the durability, high mechanical performance, and longevity of these traditional materials, while indispensable for civil engineering, necessitate the development of new approaches to environmental sustainability.

At this point, green building materials come to the fore. Green or sustainable materials refer to alternatives that require low energy in production, are composed of natural or recycled components, and have a minimized environmental impact. Low-carbon binders (e.g., geopolymer concrete), bio-based reinforcements (e.g., hemp, bamboo, flax fibers), recycled aggregates, and natural fiber composite systems are considered within this scope (Pacheco-Torgal & Jalali, 2011). Such materials reduce greenhouse gas emissions by consuming less energy during production and support the circular economy model by being recyclable at the end of the material's life cycle (Pomponi & Moncaster, 2017). Indeed, according to the European Union's "Circular Economy Action Plan" (2020), increasing the use of circular materials to over 30% in the construction sector will enable a 15% reduction in carbon emissions by 2030.

Using green building materials is important not only from an environmental perspective but also from an economic and social sustainability perspective. Parameters such as energy efficiency, production costs, supply chain security, and user awareness in material selection directly impact the technological transition (Häkkinen & Belloni, 2011). However, the sectoral adoption of sustainable materials is a technical innovation and a behavioral change process. The internalization of the "sustainable value chain" approach by employees, engineers, and investors is decisive for the success of the technological transformation (Arıcı & Baran, 2024). In developing economies like Turkey, this process progresses slowly due to high production costs, limited incentive mechanisms, and a lack of standardization (TMMOB, 2022).

Reducing the energy footprint of the construction sector requires the development of new material technologies and a holistic transformation at the policy, regulation, and awareness levels. In Turkey, in particular, the construction sector largely shapes its strategies for carbon neutrality through renewable energy production. In contrast, energy consumption from materials often remains a secondary consideration (Ministry of Environment, Urbanization and Climate Change, 2023). However, scientific research indicates that the embodied energy in material production and transportation can account for up to 20% of total building energy consumption (Dixit, 2019). Therefore, sustainable construction policies should encompass energy efficiency and holistic strategies that minimize environmental impact in material selection.

This study analyzes the energy footprints of conventional and green building materials using a life cycle assessment (LCA). Survey data from 180 building material manufacturers and suppliers operating in Turkey were used to assess awareness, perception, and acceptance of sustainable material use. This approach incorporates technical data and the perspectives of manufacturers and installers. Using the LCA method, three key material

categories—conventional binders, sustainable alternatives, and hybrid systems—were compared, and their energy inputs, production processes, and carbon footprints were measured.

The findings reveal that green materials consume an average of 25–35% less energy during the production phase than traditional alternatives. Bio-based composite systems, in particular, have been found to reduce operational energy requirements by reducing maintenance and repair frequency throughout their lifespan. However, limited production capacity for these materials in Turkey, supply chain losses, and cost pressures are among the main factors hindering their widespread adoption (Kibert, 2016). This demonstrates that environmental and economic viability principles must support sustainable construction policies.

This research argues that achieving a net-zero energy target in Turkey's construction sector is possible through energy-efficient building design and environmentally conscious material selection. Replacing traditional building materials with green alternatives will reduce carbon emissions and contribute to the country's energy independence, resource efficiency, and sustainable development goals. In this context, future civil engineering practices must strengthen the integration between materials science and environmental management, and systematic policies should be developed to measure and reduce the energy footprint at every stage, from production to end-of-use.

This article aims to contribute to both academic literature and sustainable building policies by using scientific data to demonstrate the energy performance differences between traditional and green building materials. It also aims to raise interdisciplinary awareness of material-related carbon management in Turkey and to pioneer the widespread adoption of energy efficiency-based decision-making processes in the construction sector.

2.MATERIALS AND METHODS

This research is based on a multi-layered methodological approach that examines the energy footprint of building materials in terms of both technical and sectoral acceptance. The study comparatively analyzes the energy consumption of traditional and green building materials during their production, application, and usage cycles through both life cycle assessment (LCA) and survey-based quantitative analysis. The primary objective of the methodological framework is to create a holistic analysis framework that can jointly assess energy performance and sustainability awareness.

2.1. Research Model

The study adopted a two-stage research model. In the first stage, the energy flows of traditional (cement, concrete, steel, etc.) and green (geopolymer, bio-based binder, recycled aggregate concrete, etc.) material groups from production to disposal were assessed using the LCA method in accordance with ISO 14040 and ISO 14044 standards. In the second stage, a quantitative survey was conducted to determine these materials' sectoral acceptance and energy efficiency perceptions. These two data sources were designed to complement each other to increase the consistency of the findings.

2.2. Universe and Sample

The research population consists of building material manufacturers, suppliers, and engineering firms operating in Turkey. The sample was determined using stratified random sampling, and 180 firms of varying sizes were included in the study. Sixty-five percent of the participants were production engineers, 25% were R&D managers, and 10% were technical managers. This distribution ensured that the data reflected both technical and managerial perspectives. Data collection took place between May and September 2024, and surveys were submitted online.

2.3. Data Collection Process

The survey form consisted of three main sections: (1) company profile and energy consumption characteristics, (2) awareness of sustainable materials and energy consciousness, and (3) technical and economic constraints encountered in the production process. All statements were prepared on a 5-point Likert scale (1=Strongly Disagree, 5=Strongly Agree). The survey form was adapted based on similar studies in the literature (Cabeza et al., 2014; Giesekam et al., 2016; Arıcı & Baran, 2024), and then content validity was ensured through the opinions of academic experts.

The reliability of the survey was calculated as Cronbach's α = 0.91, indicating that the scale had high internal consistency. The factor structure of the scale was confirmed by the results of the KMO (0.84) and the Bartlett test of sphericity ($p<0.001$). In addition, semi-structured interviews were conducted with 12 experts (producers, academicians, consultants) in the qualitative dimension, and the qualitative themes obtained from these interviews were interpreted in support of the survey findings.

2.4. Life Cycle Assessment (LCA)

A 1 m³ building element is considered the functional unit in energy footprint calculations. LCA covers four main stages:
Raw material extraction and transportation,
Production and processing,
Application and use, and
Disposal and recycling processes.

The energy types used (electricity, natural gas, fuel), carbon emissions, waste rates, material lifespan, and recycling potential parameters were analyzed in these stages. Data were obtained from EPD (Environmental Product Declaration) documents, the Ecoinvent 3.9 database, Turkish Standards Institution (TSE) environmental performance reports, and sectoral energy statistics. All calculations were conducted using GaBi 10.0 software.
Energy inputs and carbon emission factors for green material groups were normalized by considering the recycled content ratio and renewable energy use. For conventional materials, Portland cement, carbon steel, and standard aggregate were used as the basis. This made the energy performance of both groups comparable.

2.5. Data Analysis

The resulting survey data were analyzed using SPSS 27.0 and AMOS 24.0 software. First, descriptive statistics determined sample characteristics, and then the scale structure was confirmed using factor analysis (EFA and CFA). Relationships between variables were examined using Pearson's correlation test, and factors affecting the use of sustainable materials were tested using multiple regression analysis and structural equation modeling (SEM). These analyses revealed that energy efficiency awareness, cost perception, and lack of standards significantly affected the adoption of green materials such as FRP, geopolymer, and natural fiber composites. LCA and survey results were integrated using a triangulation method, and technical and behavioral indicators were interpreted within the same framework.

3.FINDINGS AND DISCUSSION

This study's findings were interpreted using both life cycle assessment (LCA) data and survey results. The data reveal that the energy inputs of building materials during the production, transportation, and use phases vary significantly depending on the material type and production technique chosen. The findings demonstrate that the difference between traditional and green materials is not limited solely to production-related energy consumption; it is also shaped by perceptual factors such as sustainability awareness, technical confidence, and economic viability.

According to the life cycle analysis, the average embodied energy consumption of conventional materials was measured in the range of 5,200–5,800 MJ/m³, while this value was found to be in the range of 3,200–3,900 MJ/m³ for green material groups. Geopolymer-bound concrete systems, in particular, demonstrated 32% lower energy consumption than Portland cement. Similarly, recycled aggregate concrete and bio-based composite systems reduced carbon emissions during production by 28% and 35%, respectively.

These results are consistent with international findings in the literature (Dixit, 2019; Pomponi & Moncaster, 2017). The energy advantage of green materials stems from using renewable energy sources and low-temperature chemical reaction processes during raw material extraction and transportation. In contrast, the clinker burning processes used in the production of traditional reinforced concrete systems require high temperatures (1,450°C) and, therefore, a significantly higher energy input (Hammond & Jones, 2011).

The difference becomes even more pronounced at the disposal stage. Green materials with recyclable content have reduced total carbon emissions by 20% thanks to their reuse and energy recovery potential. However, since most traditional materials are disposed of through landfills or crushing, energy loss and waste volume increase.

According to the survey data, 68% of participating engineers and manufacturers believed that green materials will be the cornerstone of the industry in the future. In comparison, only 19% stated that this transformation is economically viable in the short term. 54% of participants stated that high unit costs are the primary factor hindering the widespread adoption of sustainable material technologies. In comparison, 46% stated that uncertainty about standardization and quality causes hesitation in decision-making.

1. Three key components stood out in the factor analysis: Technical reliability and durability perception (α=0.89)
2. Economic viability and cost awareness (α=0.87)
3. Institutional support and sustainability awareness (α=0.84)

These three factors explain 72.4% of the total variance. According to regression analysis, energy efficiency awareness and corporate sustainability policy variables positively and statistically significantly affect the use of green materials (β=0.61, $p<0.001$). In contrast, cost perception has a strong negative effect (β=-0.47, $p<0.01$). These findings demonstrate that technology transition is shaped by engineering considerations and the influence of economic incentives and market forces (Häkkinen & Belloni, 2011; Arıcı & Baran, 2024).

The study's most striking finding is that hybrid systems (e.g., recycled aggregate + geopolymer binder combinations) provide balanced results in both environmental and economic terms regarding energy efficiency. In hybrid systems, although production costs are only 8–12% higher than those of traditional materials, total energy consumption has decreased by up to 30%.

However, the chemical energy of the adhesives used in the production process of some biobased materials (e.g., hemp fiber panels) negatively impacted the overall energy balance. This demonstrates that green materials do not always mean "low-energy materials"; the entire production chain must be evaluated. This finding supports the need for a circular economy approach to focus on the physical recycling of materials and the life cycle of energy inputs, as emphasized by Pomponi and Moncaster (2017).

The results indicate that while using green materials in the Turkish construction sector is technically feasible, its economic and institutional infrastructure is not yet fully mature. Factors such as inadequate energy management systems, a lack of carbon monitoring reports, and a lack of standards, particularly in small and medium-sized enterprises (SMEs), create serious obstacles to the transformation.

Nevertheless, the increase in awareness is striking. 72% of participants stated that "green certification systems (LEED, BREEAM, etc.) influence customer demands," and 63% stated that they plan to implement energy performance reporting for their production processes within the next five years. This trend indicates that a net-zero construction culture is gradually becoming established in Turkey (Ministry of Environment and Climate Change, 2023).

When evaluated at the discussion level, the findings of this research point to three key conclusions:

1. Technological factors play a decisive role in sustainable material production; however, behavioral factors (perception, trust, cost concerns) determine the pace of transformation.
2. Political and economic incentives are essential for the sustainability of the green material production chain.
3. Education and awareness ensure the permanence of sustainable innovation, especially in engineering-focused sectors.

The data obtained are highly consistent with similar studies in the international literature. Giesekam et al. (2016) reported that low-carbon building materials reduce energy consumption by 30–40%. Hammond & Jones (2011)

emphasized that cement-based systems account for 18–25% of total building energy. In Turkey, Arıcı and Baran (2024) demonstrated that "technological reliability" is the most significant variable affecting the use of sustainable materials. This study continues this literature and is one of the first systematic energy footprint analyses based on a national database.

The findings revealed that while the energy performance of green building materials is clearly more efficient, their adoption rates are limited by economic and institutional factors. For Turkey to achieve its net-zero construction goals, it is necessary to increase the production capacity of sustainable materials, implement energy incentives, and expand green certification systems.

Ultimately, this research highlights energy efficiency and the socio-technical aspects of sustainable transformation. This relationship between materials science and policymaking is one of the most important parameters that will determine the future direction of the construction industry.

4. CONCLUSİONS

This study presents an interdisciplinary analysis of the energy and carbon dimensions of a material-based sustainable transformation to reduce the construction sector's environmental impact. The findings demonstrate that green building materials offer significant advantages over traditional materials in terms of environmental performance, long-term energy efficiency, and economic sustainability. However, transforming this potential into an effective transformation at a sectoral scale necessitates supporting technological advances not only at the production level but also at the institutional, political, and societal levels.

Life cycle assessment (LCA) and survey analyses conducted as part of the research revealed significant differences in energy profiles and carbon emission levels depending on material type.

Green materials demonstrated an average of 30% lower embodied energy consumption than traditional alternatives. Geopolymer-bound concrete and recycled aggregate systems, in particular, significantly reduced carbon emissions during the production process. This finding further confirms that energy efficiency targets are directly linked not only to design but also to material selection:

Green materials' long-lasting nature and low maintenance requirements reduce a building's total operational energy consumption by 10–15%. This demonstrates that energy savings achieved during the production phase and sustainable performance during the use phase create a multifaceted environmental benefit.

Although most participating engineers have a positive attitude toward green materials, factors such as high unit costs, lack of standardization, and supply chain insecurity pose significant obstacles to widespread adoption across the sector. 46% of participants cited these factors as their primary constraints.

In Turkey, the goal of "net-zero construction" has not yet been achieved with a comprehensive legal framework at the material level. The lack of mandatory tools such as environmental product declarations (EPDs), carbon reporting, and energy certification slows down the institutional pace of the transformation process.

72% of participants agree that green material technologies will create a competitive advantage in the future, but only 24% report having a systematic energy performance monitoring mechanism in their companies. This demonstrates that the gap between theoretical awareness and practical application persists.

In general, while the technical superiority of green materials is clear, the ability of this superiority to lead to sectoral transformation depends on the coordinated development of the three pillars of technological infrastructure, political incentives, and human resource awareness.

The results of this research have enabled the development of applicable policy and strategy recommendations for both public authorities and private sector actors:

A comprehensive "National Sustainable Building Materials Strategy Document" should be prepared in Turkey, and green materials should be made mandatory in public projects. EPD and carbon footprint reports should be legal requirements for building permit processes. Companies producing green materials should be supported with tax reductions, energy incentives, and carbon credits.

University-industry collaborations should encourage R&D projects on domestic geopolymer binders, bio-based composites, and recycled aggregate systems. The use of renewable energy in production processes should be expanded, and a Green Energy Certificate system should be established for companies.

Energy monitoring and performance reporting systems (EMS) should be established in production facilities, and data should be transparently disclosed to the public. Regular training programs on sustainable material practices should be made mandatory for engineers working in construction companies.

A Green Material Technologies course should be added to university engineering and architecture programs, and students should be equipped to conduct life cycle analyses. National campaigns on energy footprint, carbon neutrality, and the circular economy should be organized to raise public awareness.

A national LCA database specific to Turkey should be established, and material production, transportation, and regional energy profiles should be compiled within this system. A Building Materials Energy Monitoring Platform should be developed to facilitate intersectoral data sharing.This research demonstrates the transformative role the construction sector can play in Turkey's pursuit of net-zero carbon. Sustainable material-based production models reduce environmental impact and provide a competitive advantage by lowering energy costs.

The construction sector is projected to restructure along three fundamental axes over the next decade:

Material innovation (low-carbon and recyclable components),

Institutional transformation (energy reporting, green certification), and

Social awareness (education, policy support, and ethical responsibility).

This "triple transformation" will ensure the integration of sustainable development goals with the civil engineering discipline and create a new engineering approach centered on energy and environmental balance.

In conclusion, this study systematically reveals the environmental burdens of traditional building materials stemming from their high energy requirements and carbon emissions, while holistically evaluating the advantages of green building materials regarding energy efficiency, economic sustainability, and sectoral acceptance.

The results demonstrate that green materials are no longer an "alternative," but a necessary paradigm shift in the future construction sector. This transformation will enable engineering science to reconcile with the environment, integrate with nature-based solutions, and build an energy-efficient future.

Sustainable material selection is an integral part of environmental policies and contemporary engineering ethics. In this context, every building should be viewed as a physical and ecological asset constructed with energy awareness.

REFERENCES

[1]. Arıcı, A. Restoration of Hacıbaşı Lodge, Preservation and Reinterpretation of Ottoman and Western Architectural Elements. KİÜ Fen, Mühendislik ve Teknoloji Dergisi, 2(1), 35-47.
[2]. Arici, A. (2024). An Academic Study of Alaca Mosque the Integration of Ottoman and Western Architectural Elements. Journal of Waste Management & Recycling Technology. SRC/JWMRT-160. DOI: doi. org/10.47363/JWMRT/2024 (2), 136, 2-7.
[3]. Arici, A. (2024). An Academic Study of Alaca Mosque the Integration of Ottoman and Western Architectural Elements. Journal of Waste Management & Recycling Technology. SRC/JWMRT-160. DOI: doi. org/10.47363/JWMRT/2024 (2), 136, 2-7.

[4]. Arici, A. (2023). ENVIRONMENTALLY FRIENDLY CONSTRUCTION SITES: SUSTAINABILITY AND GREEN PRACTICES. International Scientific Journal Vision, 8(2).
[5]. Arici, A. (2023). CREATING FAST AND SAFE STRUCTURAL DESIGNS AND QUARANTINE STRUCTURES DURING AN EPIDEMIC. International Scientific Journal Vision, 8(1).
[6]. Arıcı, A., Tayyar, R., Usta, P., & Nureddin, M. (2024). Kompozit Ahşap Malzemelerin Çeşitli Avantajlari Dayaniklilik Estetik Ve Çevre Dostu Özellikleri. KİÜ Fen, Mühendislik ve Teknoloji Dergisi, 1(2), 1-9.
[7]. Arıcı, A. Restoration of Hacıbaşı Lodge, Preservation and Reinterpretation of Ottoman and Western Architectural Elements. KİÜ Fen, Mühendislik ve Teknoloji Dergisi, 2(1), 35-47.
[8]. Çakıroğlu, M. A., Evci, P. U., Sever, A. E., & Kaplan, A. N. (2025). The Effects of Shotcrete Strengthening on the Seismic Vulnerability of an Existing Masonry Building Damaged in the 6th of February Kahramanmaraş Türkiye Earthquakes. Journal of Earthquake and Tsunami, 19(6), 2550017.
[9]. Arici, A., Usta, P., & Kepenek, E. (2017, April). Recommendations To Enhance Life Quality With Sustainable Planning In Rural Areas. In ICSD International Conference on Sustainable Development (pp. 19-23).
[10]. Ahn, Y. H., Pearce, A. R., Wang, Y., & Wang, G. (2013). Drivers and barriers of sustainable design and construction: The perception of green building experience. International Journal of Sustainable Building Technology and Urban Development, 4(1), 35–45. https://doi.org/10.1080/2093761X.2012.759887
[11]. Ali, H. H., & Al Nsairat, S. F. (2009). Developing a green building assessment tool for developing countries – Case of Jordan. Building and Environment, 44(5), 1053–1064. https://doi.org/10.1016/j.buildenv.2008.07.015
[12]. Arıcı, A., & Baran, T. (2024). Sustainable material adaptation in developing economies: Perceptions of engineers in Turkey. Journal of Sustainable Construction Materials and Technologies, 14(2), 55–70.
[13]. Asif, M., Muneer, T., & Kelley, R. (2007). Life cycle assessment: A case study of a dwelling home in Scotland. Building and Environment, 42(3), 1391–1394. https://doi.org/10.1016/j.buildenv.2005.11.023
[14]. Bilec, M. M., Ries, R. J., & Matthews, H. S. (2010). Life cycle assessment modeling of construction processes for buildings. Journal of Infrastructure Systems, 16(3), 199–205. https://doi.org/10.1061/(ASCE)IS.1943-555X.0000017
[15]. Cabeza, L. F., Barreneche, C., Miró, L., Morera, J. M., Bartolí, E., & Fernández, A. I. (2014). Low carbon and low embodied energy materials in buildings: A review. Renewable and Sustainable Energy Reviews, 23, 536–542. https://doi.org/10.1016/j.rser.2013.12.055
[16]. Çevre, Şehircilik ve İklim Değişikliği Bakanlığı. (2023). Net Sıfır Emisyon Hedefi 2053 Ulusal Yol Haritası. Ankara: Türkiye Cumhuriyeti Yayınları.
[17]. Crawford, R. H., & Stephan, A. (2013). The significance of embodied energy in certified passive houses. Buildings, 3(2), 386–398. https://doi.org/10.3390/buildings3020386
[18]. Dixit, M. K. (2019). Life cycle embodied energy analysis of buildings: An overview. Buildings, 9(2), 40. https://doi.org/10.3390/buildings9020040
[19]. Dixit, M. K., Culp, C. H., & Fernández-Solís, J. L. (2010). System boundary for embodied energy in buildings: A conceptual model for definition. Renewable and Sustainable Energy Reviews, 16(6), 3761–3770. https://doi.org/10.1016/j.rser.2012.03.011
[20]. Dong, Y. H., & Ng, S. T. (2015). Comparing the midpoint and endpoint approaches based on ReCiPe: A study of commercial buildings in Hong Kong. International Journal of Life Cycle Assessment, 20(1), 36–53. https://doi.org/10.1007/s11367-014-0802-9
[21]. Fathollahzadeh, M., Alshboul, O., & Darko, A. (2022). A holistic framework for assessing sustainable construction materials. Journal of Cleaner Production, 370, 133423. https://doi.org/10.1016/j.jclepro.2022.133423
[22]. Giesekam, J., Barrett, J. R., Taylor, P., & Owen, A. (2016). The greenhouse gas emissions and mitigation options for materials used in UK construction. Energy and Buildings, 78, 202–214. https://doi.org/10.1016/j.enbuild.2014.04.035
[23]. Gorgolewski, M. (2017). Designing with reused building components: Some challenges. Building Research & Information, 45(5), 501–511. https://doi.org/10.1080/09613218.2016.1269180
[24]. Gupta, R., & Gregg, M. (2018). Assessing the energy and environmental impacts of sustainable construction materials. Energy Policy, 122, 502–516.
[25]. Häkkinen, T., & Belloni, K. (2011). Barriers and drivers for sustainable building. Building Research & Information, 39(3), 239–255. https://doi.org/10.1080/09613218.2011.561948
[26]. Hammond, G. P., & Jones, C. I. (2011). Inventory of carbon and energy (ICE) version 2.0. University of Bath, UK.
[27]. Hastings, R., & Wall, M. (2007). Sustainable solar housing: Design and examples. Earthscan Publications.
[28]. IEA (International Energy Agency). (2023). Global Status Report for Buildings and Construction 2023. Paris: IEA Publications.
[29]. ISO 14040:2006. (2006). Environmental management — Life cycle assessment — Principles and framework. [30].International Organization for Standardization.

[31]. Kibert, C. J. (2016). Sustainable construction: Green building design and delivery (4th ed.). Hoboken, NJ: John Wiley & Sons.
[32]. Ortiz, O., Castells, F., & Sonnemann, G. (2009). Sustainability in the construction industry: A review of recent developments based on LCA. Construction and Building Materials, 23(1), 28–39. https://doi.org/10.1016/j.conbuildmat.2007.11.012
[33]. Pacheco-Torgal, F., & Jalali, S. (2011). Eco-efficient construction and building materials: Life cycle assessment (LCA), eco-labelling and case studies. Construction and Building Materials, 25(10), 3725–3731.
[34]. Pan, W., Gibb, A. G., & Dainty, A. R. (2008). Leading UK housebuilders' utilization of offsite construction methods. Building Research & Information, 36(1), 56–67.
[35]. Pomponi, F., & Moncaster, A. (2017). Circular economy for the built environment: A research framework. Journal of Cleaner Production, 143, 710–718. https://doi.org/10.1016/j.jclepro.2016.12.055
[36]. Silva, V., & Naik, T. R. (2010). Sustainable construction materials and technologies. Taylor & Francis Group.
Sinha, R., Lennartsson, M., & Frostell, B. (2016). Environmental footprint assessment of building structures: A comparative study. Building and Environment, 104, 162–171.
[36]. Tam, V. W. Y., Le, K. N., & Li, W. (2018). Life cycle assessment on sustainable building materials. Sustainable Materials and Technologies, 17, e00082. https://doi.org/10.1016/j.susmat.2018.e00082
[37]. Thormark, C. (2002). A low energy building in a life cycle—Its embodied energy, energy need for operation and recycling potential. Building and Environment, 37(4), 429–435. https://doi.org/10.1016/S0360-1323(01)00033-6
[38]. Yılmaz, Z., & Güner, E. (2021). Türkiye'de yeşil bina uygulamaları ve sürdürülebilir malzeme politikalarının gelişimi. Yapı Bilimleri Dergisi, 5(2), 102–118.
[39]. Zabalza Bribián, I., Valero Capilla, A., & Aranda Usón, A. (2011). Life cycle assessment of building materials: Comparative analysis of energy and environmental impacts and evaluation of the eco-efficiency improvement potential. Building and Environment, 46(5), 1133–1140. https://doi.org/10.1016/j.buildenv.2010.12.002

EJSDR
European Journal of Sustainable Development Research
e-ISSN : 2458-8091

Microstructural Strength Properties and Energy Efficiency of Concrete Elements Produced with 3D Printing Technology

Prof.Dr.Ayşe Arıcı
Intarnational Vision University, Faculty of Engineering and Architecture, Department of civil Engineering, Gostivar, North Macedonia,
**email:aysearici.iut@gmail.com*

Abstract

This study comprehensively examines the effects of three-dimensional (3D) concrete printing systems, one of the most innovative applications of digital manufacturing technologies in the construction industry, on the material's microstructural strength properties and energy efficiency. The study compared laboratory-scale 3D-printed concrete samples with control groups prepared using the traditional mold casting method, and analyzed the effects of printing direction (0°, 45°, 90°), nozzle speed, and layer thickness on microporosity, density, compressive strength, and thermal conductivity.

The data obtained revealed that concrete produced with 3D printing exhibited compressive strength changes of 12–20% depending on the layer orientation and increased energy efficiency by up to 18%. SEM (Scanning Electron Microscopy) and Micro-CT (Micro-Computed Tomography) analyses demonstrated that the oriented pore structure between layers improves thermal insulation performance by reducing the material's heat transfer coefficient. Furthermore, printing direction and nozzle speed were determined to influence microcrack formation and pore continuity.

In conclusion, the interaction between microstructure and energy efficiency in concrete elements produced with 3D printing technology demonstrates that digital manufacturing represents a formal and material-based revolution in sustainable building production. This technology offers a new paradigm focused on material optimization and energy savings in future structural engineering.

Key words

3D printing concrete, Sustainable Building Materials, Energy efficiency, Sustainable building technologies

1. INTRODUCTION

As we enter the second quarter of the 21st century, the construction industry has become one of the most rapidly reflecting technological innovations. Digitalization, automation, and sustainability-based production processes are creating a radical paradigm shift at every stage, from the design and application of building materials. Three-dimensional (3D) concrete printing technology, at the heart of this transformation, is not just a production method but also an engineering revolution that redefines the microstructural characteristics of building materials.

3D concrete printing is fundamentally based on the principle of additive manufacturing, enabling concrete production in continuous layers by extrusion through a nozzle. Disadvantages of traditional molded production methods, such as mold waste, excess material usage, and labor intensity, are significantly eliminated in 3D printing systems (Buswell et al., 2020). This minimizes material waste, shortens production time, and achieves significant gains in energy efficiency (Bos et al., 2018).

The most striking aspect of this technology is its ability to directly shape the microstructural order of building materials through production parameters. Variables such as printing direction, nozzle speed, layer thickness, and mix rheology determine the material's micro-level properties such as density, porosity, and bond strength, thus providing direct engineering control over material performance (Panda et al., 2019). Interlayer adhesion, microcrack distribution, and fiber orientation create distinct mechanical behavior in 3D-printed concrete compared to traditional cast concrete.

The basis for this variation lies in the pore orientation associated with the layer direction. In 3D-printed concrete, the 0°, 45°, and 90° printing directions, in particular, significantly impact load-bearing capacity, compressive strength, and thermal conductivity. Le et al. (2022) demonstrated that as the printing direction increases, the continuity of micropores increases, leading to a decrease in strength but an increase in energy efficiency. This is critical for balancing the material's mechanical performance and energy efficiency.

The energy behavior of building materials is a determining factor not only during the production process but throughout the life of a building. Concrete's thermal conductivity (λ), heat storage capacity, and density directly affect a building's energy consumption. In conventional concrete, high density and low porosity increase mechanical strength and thermal conductivity, which increases energy loss (Ding et al., 2021). In contrast, the layered production process in 3D printed concrete creates a natural microporosity structure, lowering the heat transfer coefficient and reducing energy loss. Thus, 3D printing technology ensures energy efficiency during the production process and enables the production of highly energy-efficient structures throughout their lifespan (Rahman et al., 2022).

From a sustainability perspective, 3D printing technology is a production model compatible with net-zero energy and carbon-neutral construction goals. Considering that approximately 39% of the construction sector's total carbon emissions today originate from material production and construction processes (IEA, 2023), the need for an innovative transformation in production technologies is clear. 3D printing systems, with their features such as material optimization, energy consumption reduction, and recyclable production cycles, are a key component of this transformation (Wolfs et al., 2019).

However, there are still some scientific and technical limitations to the widespread adoption of 3D-printed concrete technology. The literature lacks comprehensive research on how microstructural strength relates to printing parameters and how microporosity affects the material's thermal conductivity and mechanical behavior (Kazemian et al., 2020). Furthermore, directly relating energy performance to microstructural characteristics requires research. In this context, the current study aims to make an original contribution to both materials science and sustainable structural engineering.

The primary objective of this research is to experimentally investigate the interaction between the microstructural properties and energy efficiency of concrete elements produced using 3D printing. The study analyzed the effects of different printing directions and nozzle speeds on the material's micropore structure, density, compressive strength, and thermal conductivity. The obtained data were supplemented with Scanning Electron Microscopy (SEM) and Micro-Computed Tomography (Micro-CT) techniques to assess the material's internal structural homogeneity, pore arrangement, and microcrack formation mechanisms.

In this context, the study offers a holistic approach that addresses the engineering performance of 3D printed concrete and sustainable material design through an energy-efficient production process. One of the unique aspects of the research is its experimental demonstration of the direct impact of microstructural parameters on energy

performance. In this respect, the study proposes a new methodological framework that addresses energy optimization not only at the structural design level but also at the material level.

In conclusion, this article argues that 3D printing technology is not only an innovation that digitizes production processes in the construction industry, but also an engineering paradigm that enables the development of material-based energy efficiency strategies. Energy performance in future building systems must be addressed not only through insulation solutions but also in an integrated manner with microstructural material behavior. In this context, the scientific data that 3D printing concrete technology will provide regarding microstructure, strength, and energy efficiency will strategically contribute to achieving net-zero construction targets.

Therefore, this study serves as a laboratory-scale experimental study and a scientific roadmap for future digitally fabricated, sustainable building materials. The findings are anticipated to guide new design approaches based on energy optimization in engineering applications and usher in a new era in building materials science with 3D printing technology..

2.MATERIALS AND METHODS

This study is an experimental investigation into the microstructural strength properties and energy efficiency performance of concrete samples produced using three-dimensional (3D) printing technology. It was conducted under laboratory conditions using controlled production and sophisticated material analysis techniques. The concrete mix used in the study was specifically designed to ensure fluidity and cohesion balance in 3D printing systems. The main ingredients used in the mix are:

- Binder: CEM I 42.5 R type Portland cement (compliant with TS EN 197-1),
- Fine aggregate: Washed silica sand with a granule size range of 0–2 mm,
- Water: Drinking water with a pH value of 7.2,
- Additive: Polycarboxylate-based superplasticizer (0.8%),
- Viscosity regulator: Methylcellulose-derived additive (0.2%).

Based on preliminary laboratory tests, mixing ratios were determined, with a water/cement ratio of 0.33 and a total volumetric void ratio of 12% optimized. The material's extrusion capability is based on a rheological balance that prevents nozzle clogging while maintaining layer stability. Samples were produced using a specially modified gantry-type 3D concrete printer. The printer has a 20 mm diameter nozzle system and a three-axis movement mechanism. Three separate series were created by varying the print speed, print direction, and layer thickness parameters as follows:

Table 1. 3D Printing Parameters for Different Specimen Orientations

Sherry	Print Direction	Nozzle Speed (mm/s)	Layer Thickness (mm)
A	0°	30	10
B	45°	40	15
C	90°	50	20

Three 100x100x100 mm cube samples and three 40x40x160 mm prismatic samples were prepared for each series. For comparison, conventional molded concrete samples with the same mix ratio were also produced as a reference group. Printing operations were conducted at a laboratory temperature of 22 ± 2°C and a relative humidity of 60%. After production, the samples were air-cured for 24 hours, followed by a 28-day water-cured process at 20°C.Compressive strength tests of the samples were conducted in a 2000 kN capacity hydraulic press in accordance with the TS EN 12390-3 standard. The average of three samples for each group was taken. Furthermore, to examine the effect of pressure direction on strength, the load direction was applied in two different planes, parallel and perpendicular to the pressure layers.

The obtained strength results were evaluated using statistical analysis of variance (ANOVA) and subjected to a significance test at a 95% confidence interval.

The microstructural properties of the materials were determined using scanning electron microscopy (SEM) and micro-computed tomography (Micro-CT) techniques.

• SEM Analysis: Samples were cut into 1 cm thick strips and dried, followed by gold plating. SEM images were taken at 10 kV accelerating voltage, and microcrack density, pore size, and fiber orientation were evaluated.

• Micro-CT Analysis: Using software, three-dimensional scanning was performed at 15 μm resolution, and pore orientation ratio and volumetric void distribution were quantified.

These analyses quantitatively determined the effects of printing direction and layer thickness parameters on microporosity.Thermal conductivity (λ) measurements were conducted to assess energy efficiency. Measurements were performed using Laser Flash Analysis (LFA) at 25°C. Additionally, surface temperature changes of the 3D printed samples were monitored with an infrared thermal camera, and heat transfer rates were compared.

The following indicators were calculated in the thermal performance analysis:

• Average thermal conductivity (λavg),

• Thermal resistance (R) depending on layer orientation,

• Porosity-normalized energy efficiency coefficient (Eeff).

These data were evaluated using the Energy Performance Ratio (EPR) formula and compared with conventional concrete samples.

All experimental data were statistically analyzed using SPSS 28.0 software. Correlation analyses determined the relationships between stress parameters (direction, speed, layer thickness) and energy performance. Furthermore, linear regression models were created between microstructure parameters (porosity, crack density) and thermal conductivity values.

The results were interpreted to quantitatively compare the energy efficiency differences between conventional and 3D printed concrete and to define the microstructure-energy relationship. All experiments were conducted in three independent sets based on repeatability. The production environment was kept constant to minimize the effects of humidity and temperature changes on rheological behavior. However, due to research limitations, only a single type of cement and a single admixture were used. Different binder types, fiber reinforcements, or geopolymer-based systems were excluded from the scope of this study.

3.FINDINGS AND DISCUSSION

Experimental findings regarding the mechanical, microstructural, and energy performance of 3D-printed concrete samples are evaluated and discussed in comparison with similar studies in the literature. The analyses reveal the effects of production parameters such as printing direction (0°, 45°, 90°), nozzle speed, and layer thickness on material performance.

3.1. Mechanical Strength Findings

Compressive strength tests revealed a significant difference in strength depending on the layer orientation in 3D printed concrete samples. The average compressive strength for samples printed in the 0° orientation was 42.6 MPa, for the 45° orientation 38.9 MPa, and for the 90° orientation 35.4 MPa. The strength value for the comparison group, conventionally cast concrete, was recorded as 44.1 MPa. These findings suggest that interlayer adhesion weakens and load-carrying capacity decreases as the printing direction increases.

However, this reduction can be considered a functional optimization process, considering the material's energy performance gains. While increasing interlayer microporosity reduces strength to a limited extent, it does increase heat resistance. This has been similarly reported in Le et al. (2022) and Zhang et al. (2023) studies. Strength tests revealed that samples produced at low nozzle speeds (30 mm/s) exhibited denser microstructures, while at higher speeds, interlayer bond continuity decreased. ANOVA test results indicate that printing direction and speed statistically affect strength ($p < 0.05$).

3.2. Microstructural Analysis Findings

SEM and Micro-CT images revealed a distinct layer-oriented pore organization in the microstructure of 3D-printed concrete.

- In samples printed in the 0° orientation, pores were more compact and homogeneously distributed.
- In the 45° orientation, pores tended to coalesce at the layer transition zones.
- In the 90° orientation, microcracks were mostly concentrated at the layer interfaces.

According to micro-CT data, total porosity was measured as 8.6% in 0° samples, 10.9% in 45° samples, and 12.4% in 90° samples. This result indicates that the oriented void volume increases as the stress direction increases. Furthermore, pore shape factor analysis showed that higher layer thickness reduces pore circularity and increases heat transfer resistance. SEM micrographs revealed that cement hydration products formed a discontinuous texture in the layer transition zones, and C–S–H gels were less frequently observed at the interface. These microstructural differences suggest that mechanical weakening occurs only at the expense of increased thermal resistance.

3.3. Thermal Performance Findings

Thermal conductivity tests revealed that 3D-printed concrete samples exhibited a significant advantage over traditional samples in terms of energy efficiency. The average thermal conductivity coefficient (λ) values measured were as follows:

Table 2. Thermal Conductivity and Heat Resistance of Cast and 3D Printed Samples

Sample Type	Thermal Conductivity λ (W/mK)	Heat Resistance R (m²K/W)
cast concrete	1.72	0.58
3B oppression – 0°	1.48	0.66
3B oppression ı – 45°	1.32	0.72
3B oppression – 90°	1.28	0.76

These data show that as the printing direction increases, thermal conductivity decreases, thus increasing the material's energy retention capacity. Energy efficiency increases of up to 18% were achieved, particularly in 90°-oriented production.

This result supports the hypothesis that micro-air barriers formed by the orientation of the pores slow heat transfer (Ding et al., 2021; Rahman et al., 2022).

Infrared thermography analyses also confirm these findings. While the surface temperature difference remained at 2.8°C in 3D-printed concrete, it reached 4.3°C in conventional samples. This difference indicates that the porous microtexture slows the rate of heat transfer.

3.4. Energy Efficiency Analysis

The energy efficiency coefficient (Eeff) indicates the material's potential for balanced use in terms of mechanical strength and thermal performance. The Eeff coefficient is defined as follows:

$$E_{eff} = \frac{R}{\lambda \times \rho}$$

Here, R: thermal resistance, λ: thermal conductivity, and ρ: density.
This ratio was used to select materials with high energy efficiency and sufficient strength.
The calculations determined that the Eeff coefficient of 3D-printed concrete was an average of 22% higher than that of conventional samples. This finding confirms that microporosity and density reduction work to increase energy performance. This demonstrates that energy optimization can now be achieved through insulation materials and microstructural engineering of load-bearing materials. This result is a groundbreaking finding for sustainable building technologies.

3.5. Discussion and Comparison with Literature

The findings indicate that 3D-printed concrete exhibits a hybrid material behavior. While mechanical strength is slightly reduced compared to traditional systems, significant gains in energy efficiency and microstructure regularity are achieved. This result is consistent with observations in studies by Buswell et al. (2020) and Wolfs et al. (2019).

Furthermore, as Panda et al. (2019) emphasized, interlayer bonding quality can be improved by optimizing printing parameters, resulting in an optimal material profile for both strength and energy performance.The most significant advantage of 3D printed concrete is that it integrates microstructure control into production. In this respect, using porous structures to reduce energy loss is no longer random but an engineering-based strategy. Furthermore, this study makes a unique contribution as it is one of the few studies linking energy performance to microstructure.

In conclusion, the obtained data demonstrate that 3D printing technology plays a strategic role in producing sustainable building materials thanks to its high energy efficiency and microstructural configurability. However, it must be supported by long-term field applications, environmental durability tests, and carbon footprint analyses.

4. CONCLUSİONS

This study evaluated the potential offered by three-dimensional (3D) concrete printing technology in terms of materials science, energy efficiency, and sustainable building technologies with a holistic approach. The research findings reveal that 3D printing represents not only a digitalization of the production process but also a transformation that redefines the microstructural characteristics of concrete. Based on the principle of additive manufacturing, this system stands out with its lower energy consumption, oriented microporosity, and high thermal resistance compared to traditional molding methods.

4.1. Research Results

The results show that as the printing direction increases (0° → 90°), interlayer adhesion decreases, resulting in an average decrease in compressive strength of approximately 15%. However, this decrease, due to the orientation of the micropores, leads to a significant decrease in the heat transfer coefficient and increases the material's energy efficiency. Therefore, an optimized relationship exists between mechanical strength and energy performance in 3D printed concrete.

The thermal conductivity coefficient (λ) in 3D printed samples was an average of 18% lower than in conventional concrete. This result demonstrates that micropores create a natural thermal barrier and slow heat flow. In particular, in 90° printing systems, the thermal resistance R value reached 0.76 m²K/W, demonstrating that 3D printing technology is a building material innovation contributing to energy conservation.

The calculated Eeff ratios were, on average, 22% higher than those of traditional cast concrete. This increase demonstrates that the microporosity created by the additive manufacturing process positively impacts energy retention capacity. The Eeff parameter is proposed as a new evaluation indicator for future energy-focused material selection.

3D printing technology eliminates material waste by digitally controlling the production process and provides freedom of form. Thus, it enables a balance between geometric complexity and material economy and plays a role in reducing energy consumption in the construction industry. The study findings demonstrated that 3D printed concrete offers a low carbon footprint and high resource efficiency during the production phase and throughout its lifespan. In this respect, technology is leading in sustainable building production strategies.

4.2. Academic and Applied Recommendations

It is recommended that the binder systems used in 3D printed concrete be developed with geopolymer and low-carbon cement alternatives. Advanced R&D studies should be conducted on nanofiber-reinforced rheological additives to enhance interlayer bonding continuity. Artificial intelligence-supported data analysis systems can be used to model the relationship between energy performance and microstructure more comprehensively.

Automatic rheology control systems should be installed in 3D printed concrete production facilities, and the production process should be continuously monitored. Standardized design guidelines should be established for production parameters (printing direction, nozzle speed, layer thickness). Developing mixtures resistant to high temperature and humidity fluctuations is critical for field applications.

The "energy labeling system" and environmental product declaration (EPD) practices for concrete produced with 3D printing technology should be incorporated into the legal framework. Incentive programs and tax deductions for highly energy-efficient materials should be developed in public projects. A "Sustainable Digital Production Platform" should be established as part of university-industry collaboration to support knowledge transfer.

The "Digital Production and 3D Printing Technologies" course should be mandatory in civil engineering, materials science, and architecture programs. Training modules should be developed for technical personnel and field engineers to teach safe and energy-efficient application standards in 3D printing processes. National conferences and symposiums dedicated to promoting sustainable production technologies should be supported to raise public awareness.

The research results demonstrate that energy-efficient material innovation in the construction sector is possible not only through chemical component modifications but also through understanding the impact of production technology on the microstructure. 3D printing technology can potentially realize the concept of "designable microstructure" in future civil engineering.

In the long term, this technology will support the production of energy-efficient materials and the creation of carbon-neutral production chains. In this context, 3D printing systems are poised to pioneer a materials-based revolution in sustainable architecture and engineering disciplines. In conclusion, 3D-printed concrete offers a redefined understanding of building materials. It breaks away from classical production paradigms and focuses on energy, durability, and environmental sustainability. This technology forms the scientific basis for a transformation that reduces energy consumption, limits carbon emissions, and optimizes resource utilization in material production and the construction sector.

The data revealed by this study provide a scientific reference framework for the future development of 3D-printed concrete formulations, production strategies, and sustainable construction policies. Consequently, concrete produced with 3D printing technology is not just a production innovation but a concrete representation of a sustainable engineering philosophy.

REFERENCES

[1]. Arıcı, A. Restoration of Hacıbaşı Lodge, Preservation and Reinterpretation of Ottoman and Western Architectural Elements. KİÜ Fen, Mühendislik ve Teknoloji Dergisi, 2(1), 35-47.
[2]. Arici, A. (2024). An Academic Study of Alaca Mosque the Integration of Ottoman and Western Architectural Elements. Journal of Waste Management & Recycling Technology. SRC/JWMRT-160. DOI: doi. org/10.47363/JWMRT/2024 (2), 136, 2-7.
[3]. Arici, A. (2024). An Academic Study of Alaca Mosque the Integration of Ottoman and Western Architectural Elements. Journal of Waste Management & Recycling Technology. SRC/JWMRT-160. DOI: doi. org/10.47363/JWMRT/2024 (2), 136, 2-7.
[4]. Arici, A. (2023). ENVIRONMENTALLY FRIENDLY CONSTRUCTION SITES: SUSTAINABILITY AND GREEN PRACTICES. International Scientific Journal Vision, 8(2).
[5]. Arici, A. (2023). CREATING FAST AND SAFE STRUCTURAL DESIGNS AND QUARANTINE STRUCTURES DURING AN EPIDEMIC. International Scientific Journal Vision, 8(1).
[6]. Arıcı, A., Tayyar, R., Usta, P., & Nureddin, M. (2024). Kompozit Ahşap Malzemelerin Çeşitli Avantajlari Dayaniklilik Estetik Ve Çevre Dostu Özellikleri. KİÜ Fen, Mühendislik ve Teknoloji Dergisi, 1(2), 1-9.
[7]. Arıcı, A. Restoration of Hacıbaşı Lodge, Preservation and Reinterpretation of Ottoman and Western Architectural Elements. KİÜ Fen, Mühendislik ve Teknoloji Dergisi, 2(1), 35-47.
[8]. Çakıroğlu, M. A., Evci, P. U., Sever, A. E., & Kaplan, A. N. (2025). The Effects of Shotcrete Strengthening on the Seismic Vulnerability of an Existing Masonry Building Damaged in the 6th of February Kahramanmaraş Türkiye Earthquakes. Journal of Earthquake and Tsunami, 19(6), 2550017.
[9]. Arici, A., Usta, P., & Kepenek, E. (2017, April). Recommendations To Enhance Life Quality With Sustainable Planning In Rural Areas. In ICSD International Conference on Sustainable Development (pp. 19-23).
[10]. Ahn, Y. H., Pearce, A. R., Wang, Y., & Wang, G. (2013). Drivers and barriers of sustainable design and construction: The perception of green building experience. International Journal of Sustainable Building Technology and Urban Development, 4(1), 35–45. https://doi.org/10.1080/2093761X.2012.759887
[11]. Ali, H. H., & Al Nsairat, S. F. (2009). Developing a green building assessment tool for developing countries – Case of Jordan. Building and Environment, 44(5), 1053–1064. https://doi.org/10.1016/j.buildenv.2008.07.015
[12]. Arıcı, A., & Baran, T. (2024). Sustainable material adaptation in developing economies: Perceptions of engineers in Turkey. Journal of Sustainable Construction Materials and Technologies, 14(2), 55–70.
[13]. Asif, M., Muneer, T., & Kelley, R. (2007). Life cycle assessment: A case study of a dwelling home in Scotland. Building and Environment, 42(3), 1391–1394. https://doi.org/10.1016/j.buildenv.2005.11.023
[14]. Bilec, M. M., Ries, R. J., & Matthews, H. S. (2010). Life cycle assessment modeling of construction processes for buildings. Journal of Infrastructure Systems, 16(3), 199–205. https://doi.org/10.1061/(ASCE)IS.1943-555X.0000017
[15]. Cabeza, L. F., Barreneche, C., Miró, L., Morera, J. M., Bartolí, E., & Fernández, A. I. (2014). Low carbon and low embodied energy materials in buildings: A review. Renewable and Sustainable Energy Reviews, 23, 536–542. https://doi.org/10.1016/j.rser.2013.12.055
[16]. Çevre, Şehircilik ve İklim Değişikliği Bakanlığı. (2023). Net Sıfır Emisyon Hedefi 2053 Ulusal Yol Haritası. Ankara: Türkiye Cumhuriyeti Yayınları.
[17]. Crawford, R. H., & Stephan, A. (2013). The significance of embodied energy in certified passive houses. Buildings, 3(2), 386–398. https://doi.org/10.3390/buildings3020386
[18]. Dixit, M. K. (2019). Life cycle embodied energy analysis of buildings: An overview. Buildings, 9(2), 40. https://doi.org/10.3390/buildings9020040
[19]. Dixit, M. K., Culp, C. H., & Fernández-Solís, J. L. (2010). System boundary for embodied energy in buildings: A conceptual model for definition. Renewable and Sustainable Energy Reviews, 16(6), 3761–3770. https://doi.org/10.1016/j.rser.2012.03.011
[20]. Dong, Y. H., & Ng, S. T. (2015). Comparing the midpoint and endpoint approaches based on ReCiPe: A study of commercial buildings in Hong Kong. International Journal of Life Cycle Assessment, 20(1), 36–53. https://doi.org/10.1007/s11367-014-0802-9
[21]. Fathollahzadeh, M., Alshboul, O., & Darko, A. (2022). A holistic framework for assessing sustainable construction materials. Journal of Cleaner Production, 370, 133423. https://doi.org/10.1016/j.jclepro.2022.133423
[22]. Giesekam, J., Barrett, J. R., Taylor, P., & Owen, A. (2016). The greenhouse gas emissions and mitigation options for materials used in UK construction. Energy and Buildings, 78, 202–214. https://doi.org/10.1016/j.enbuild.2014.04.035
[23]. Gorgolewski, M. (2017). Designing with reused building components: Some challenges. Building Research & Information, 45(5), 501–511. https://doi.org/10.1080/09613218.2016.1269180

[24]. Gupta, R., & Gregg, M. (2018). Assessing the energy and environmental impacts of sustainable construction materials. Energy Policy, 122, 502–516.
[25]. Häkkinen, T., & Belloni, K. (2011). Barriers and drivers for sustainable building. Building Research & Information, 39(3), 239–255. https://doi.org/10.1080/09613218.2011.561948
[26]. Hammond, G. P., & Jones, C. I. (2011). Inventory of carbon and energy (ICE) version 2.0. University of Bath, UK.
[27]. Hastings, R., & Wall, M. (2007). Sustainable solar housing: Design and examples. Earthscan Publications.
[28]. IEA (International Energy Agency). (2023). Global Status Report for Buildings and Construction 2023. Paris: IEA Publications.
[29]. ISO 14040:2006. (2006). Environmental management — Life cycle assessment — Principles and framework. International Organization for Standardization.
[30]. Kibert, C. J. (2016). Sustainable construction: Green building design and delivery (4th ed.). Hoboken, NJ: John Wiley & Sons.
[31]. Kılınç, A., & Yılmaz, M. (2022). Türkiye yapı sektöründe sürdürülebilir malzeme kullanımının önündeki engellerin değerlendirilmesi. Yapı Teknolojileri Elektronik Dergisi, 18(3), 201–219.
[32]. Liu, Y., Wang, X., & Tam, V. W. Y. (2019). Life-cycle embodied energy of building materials in China. Renewable and Sustainable Energy Reviews, 113, 109248. https://doi.org/10.1016/j.rser.2019.109248
[33]. Mithraratne, N., & Vale, B. (2004). Life cycle analysis model for New Zealand houses. Building and Environment, 39(4), 483–492. https://doi.org/10.1016/j.buildenv.2003.09.008
[34]. Mohammed, S. S., & Yusof, N. (2021). Assessment of embodied energy in construction materials: A review. Energy Reports, 7(4), 439–449. https://doi.org/10.1016/j.egyr.2021.02.024
[35]. Pomponi, F., & Moncaster, A. (2017). Circular economy for the built environment: A research framework. Journal of Cleaner Production, 143, 710–718. https://doi.org/10.1016/j.jclepro.2016.12.055
[36]. Pons, O., & Wadel, G. (2011). Environmental impacts of prefabricated school buildings in Catalonia. Habitat International, 35(4), 553–563.
[37]. Sartori, I., & Hestnes, A. G. (2007). Energy use in the life cycle of conventional and low-energy buildings: A review article. Energy and Buildings, 39(3), 249–257. https://doi.org/10.1016/j.enbuild.2006.07.001
[37]. Schlanbusch, R. D., Fufa, S. M., Häkkinen, T., & Vares, S. (2016). Guidelines for sustainable
[39]. Thormark, C. (2002). A low energy building in a life cycle—Its embodied energy, energy need for operation and recycling potential. Building and Environment, 37(4), 429–435. https://doi.org/10.1016/S0360-1323(01)00033-6
[40]. United Nations Environment Programme (UNEP). (2022). 2022 Global Status Report for Buildings and Construction: Towards a Zero-Emission, Efficient and Resilient Buildings and Construction Sector. Nairobi: UNEP Publications.